

| | |
|---------------------|--|
| Zeitschrift: | Schweizerische mineralogische und petrographische Mitteilungen = Bulletin suisse de minéralogie et pétrographie |
| Band: | 69 (1989) |
| Heft: | 3 |
| Artikel: | Petrology, geochemistry and metamorphic evolution of the ophiolitic eclogites and related rocks from the Sierra Nevada (Betic Cordilleras, Southeastern Spain) |
| Autor: | Puga, E. / Diaz de Federico, A. / Fediukova, E. |
| DOI: | https://doi.org/10.5169/seals-52805 |

Nutzungsbedingungen

Die ETH-Bibliothek ist die Anbieterin der digitalisierten Zeitschriften auf E-Periodica. Sie besitzt keine Urheberrechte an den Zeitschriften und ist nicht verantwortlich für deren Inhalte. Die Rechte liegen in der Regel bei den Herausgebern beziehungsweise den externen Rechteinhabern. Das Veröffentlichen von Bildern in Print- und Online-Publikationen sowie auf Social Media-Kanälen oder Webseiten ist nur mit vorheriger Genehmigung der Rechteinhaber erlaubt. [Mehr erfahren](#)

Conditions d'utilisation

L'ETH Library est le fournisseur des revues numérisées. Elle ne détient aucun droit d'auteur sur les revues et n'est pas responsable de leur contenu. En règle générale, les droits sont détenus par les éditeurs ou les détenteurs de droits externes. La reproduction d'images dans des publications imprimées ou en ligne ainsi que sur des canaux de médias sociaux ou des sites web n'est autorisée qu'avec l'accord préalable des détenteurs des droits. [En savoir plus](#)

Terms of use

The ETH Library is the provider of the digitised journals. It does not own any copyrights to the journals and is not responsible for their content. The rights usually lie with the publishers or the external rights holders. Publishing images in print and online publications, as well as on social media channels or websites, is only permitted with the prior consent of the rights holders. [Find out more](#)

Download PDF: 23.02.2026

ETH-Bibliothek Zürich, E-Periodica, <https://www.e-periodica.ch>

Petrology, geochemistry and metamorphic evolution of the ophiolitic eclogites and related rocks from the Sierra Nevada (Betic Cordilleras, Southeastern Spain)

by *E. Puga¹, A. Diaz de Federico¹, E. Fediukova², M. Bondi³ and L. Morten⁴*

Abstract

The Sierra Nevada metabasites form part of a dismembered, metamorphosed ophiolitic sheet, tectonically thrust between the ensialic nappes of the Mulhacén Group, which belong to the Sierra Nevada, or Nevado-Filábride, Complex of the Betic Cordilleras. The petrological and geochemical characteristics of four representative metabasite outcrops are described, together with their P-T-t evolution during the Alpine orogeny. They are Coleman's type C eclogites with partial transformation towards amphibolitized eclogites and, to a lesser extent, amphibolitized-omphacite felses and amphibolitized garnet glaucophanites. Their inherited textures point to cumulitic gabbros, gabbros, dolerites, porphyric and aphyric basalts as being the precursor rocks.

Major and trace elements show their tholeiitic affinity, with chemical compositions similar to those of the ophiolitic basalts from the western Mediterranean and the P-type MORB basalts.

The garnets are almandine-rich (Alm_{52-60} , Pyr_{12-24} , Spess_{2-6} , Gro_{16-29} , And_{1-5}), whereas the clinopyroxenes are omphacites with jadeite contents varying from 35% to 50%. Two types of amphiboles occur: i) eo-Alpine glaucophanes, ii) Alpine s.s. barroisites and subordinate Mg-kataphorites, hastingsites and actinolites.

Microtextural analysis and K-Ar mica dating indicate two main metamorphic events correlatable to the eo-Alpine and Lepontine events in the Alps. The first event (eo-Alpine) reached its climax in eclogite-facies conditions at around 640°C and 16 kbar. The second metamorphic event (Alpine s.s.), reached its climax at around 580°C and 9 kbar. Both events were followed by an uplift of the subducted material resulting in the development of assemblages in glaucophane-schist-facies and greenschist-facies conditions.

Keywords: Ophiolitic eclogites, metamorphic evolution, P-T-t paths, Alpine orogeny, Betic Cordillera, Nevado-Filábride Complex.

1. Introduction

Almost all amphibolite and eclogite outcrops are located in the western part of the Sierra Nevada in an area bounded by Lanjarón to the south and Lugros to the north (Fig. 1). Their presence was first reported by ZERMATTEN (1929) and later by FALLOT et al. (1967). These metabasites have since been studied in more detail by PUGA (1965, 1971), PUGA and DIAZ DE FEDERICO (1976), PUGA (1977) and DIAZ DE FEDERICO (1980).

The amphibolites and eclogites of the Sierra Nevada are associated with ultramafic rocks (serpentinites and harzburgites) containing rodingite dikes. This association is interpreted as being part of a dismembered ophiolitic sequence (PUGA and DIAZ DE FEDERICO, 1976, 1984; PUGA, 1977; BURGOS et al., 1980; BODINIER et al., 1987). The accretion of the ocean-floor must have taken place in a distensive period during the Jurassic. Some gabbroic rocks pertaining to this ophiolitic association have been dated to 140 Ma by means of Rb-Sr whole-rock isochrones

¹ Instituto Andaluz de Geología Mediterránea (CSIC - Universidad de Granada), Avda. Fuentenueva s.n., E-18002 Granada, Spain.

² Geological Survey of Czechoslovakia, Malostranske Namesti n° 19, CS-11821 Praha, Czechoslovakia.

³ Dipartimento di Scienze Mineralogiche, Università di Bologna, Piazza di Porta S. Donato, 1, I-40127 Bologna, Italy.

⁴ Dipartimento di Scienze della Terra, Università della Calabria, I-87030 Castiglione Consentino Stazione CS, Italy.

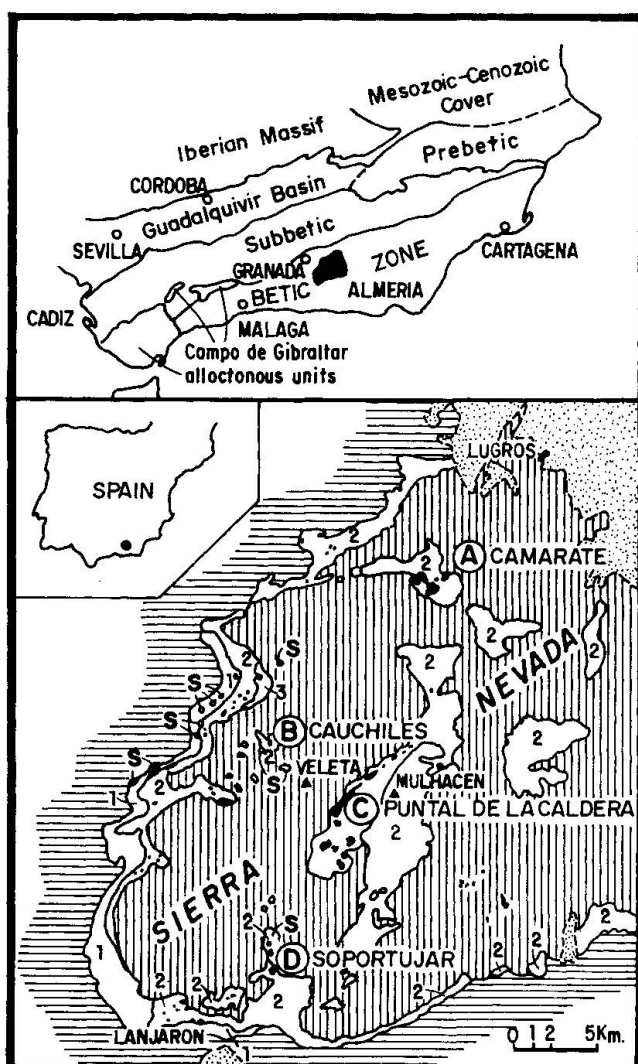


Fig. 1 Tectonic sketch map of the Sierra Nevada Complex in the central part of the Betic Cordillera, showing location of metabasite outcrops studied. Symbols: vertical lines = Veleta Group of nappes; 1, 2 and 3 = Sabinas, Caldera and San Francisco nappes of the Mulhacén Group; solid black areas = metabasites; S = serpentinites; horizontal lines = Alpujarride Complex; dotted area = post-nappe deposits.

(HEBEDA et al., 1977). In the Upper Cretaceous this ocean-floor and the partially oceanized continental crust were subducted and metamorphosed.

The intention of this work is to describe the Sierra Nevada eclogites and related rocks from both chemical and metamorphic points of view and also to compare them with similar types of rocks from the Tethyan belt.

2. Regional geology and lithology

In the Betic Cordilleras eclogites crop out only on top of the Caldera Unit of the Sierra

Nevada Complex. This high-pressure complex, originally termed Nevado-Filábride (EGELER, 1963) and later Sierra Nevada (PUGA et al., 1974), is the deepest one in the Betic Cordilleras and crops out in a tectonic window below the low-pressure Alpujarride Complex (Fig. 1).

The Sierra Nevada Complex consists of two groups of nappes: the Veleta below and the Mulhacén above (DIAZ DE FEDERICO, 1980). They in turn are composed of several tectonic units. The overthrusting of the two nappe groups must have taken place after the Alpine metamorphism since the upper group shows more intense metamorphism than the lower one (PUGA, 1971; PUGA et al., 1974).

The Sierra Nevada metabasites (Fig. 1) form part of an ophiolitic nappe tectonically intercalated between the Caldera and the Sabinas Units of the Mulhacén group of nappes. This oceanic-crust material underwent the same Alpine metamorphism and deformation as the continental-crust lithotypes forming the underlying Caldera nappe.

The most outstanding structure in the western Sierra Nevada is an antiform running approximately N40°E with its axis situated between the Veleta and Mulhacén peaks. The «Puntal de la Caldera» outcrop is located in the central part of the western Sierra Nevada close to the axis of this antiform. The «Camarate» and «Cauchiles» outcrops are on the northern slope of the Sierra Nevada and the «Soportujar» outcrop on the southern slope of the same chain. The metabasite bodies are irregular in shape and range from some hundreds of metres up to three kilometres in length (Fig. 2). They are generally not thicker than a few hundred metres. Their tectonic boundaries with the country rocks are in many places apparently concordant. Textures inherited from different protoliths such as gabbros, cumulitic gabbros, dolerites, porphyric and aphyric basalts, can be identified in all the outcrops. The transition from gabbros to basalts takes place either abruptly or over a very short distance. Sometimes metabasaltic dykes cut across both types of rock.

Antigorite-bearing harzburgitic serpentinites, relics of the ultramafic layers of this ophiolitic sequence (Fig. 2), occur in the Cauchiles and Soportujar outcrops. These rocks are locally cut by boudinaged dikes of amphibolite or rodingite, deriving from basaltic rocks. The metasedimentary rocks associated with the metabasites are mainly: epidote + garnet calc-schists with ankerite or siderite nodules, albite + amphibole micaschists, garnet ± kyanite ± chloritoid micaschists and thin beds or lenses of albite + epidote

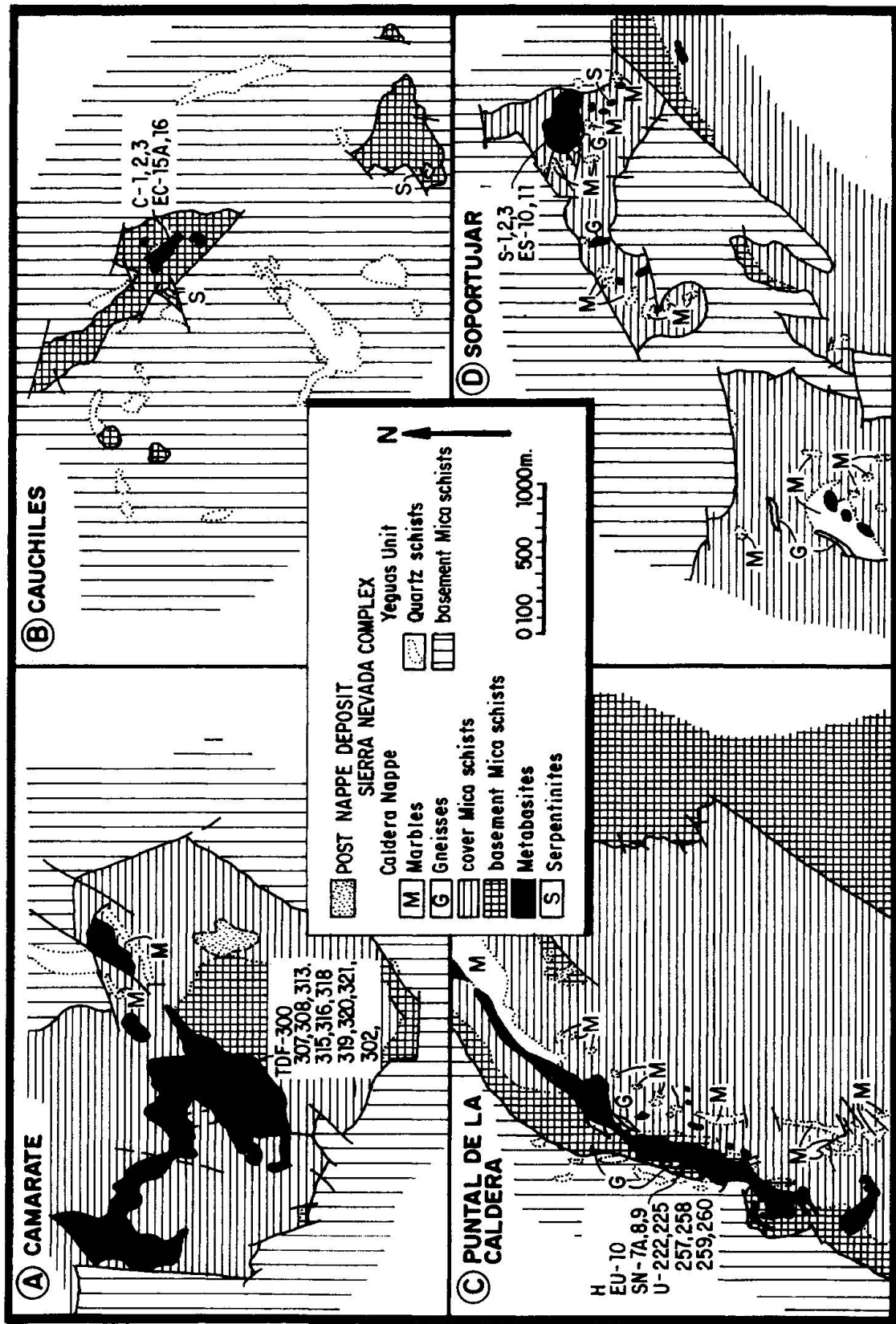


Fig. 2 Lithological sketch map of the four studied eclogite outcrops; numbers = analyzed samples.

+ white-mica-bearing marbles. They presumably formed the sedimentary cover of the ophiolitic sequence.

The following types of metabasite can be identified: amphibole-bearing eclogites (E), amphibolitized eclogites (AE), amphibolitized omphacite felses (AOF) and amphibolitized garnet-glaucophanites (AGG).

The most abundant metabasic rock type is a slightly retrograded eclogite (E) with minor quantities of glaucophane and/or Na-Ca amphibole. These type C eclogites (COLEMAN et al., 1965) formed during the older eo-Alpine event (PUGA and DIAZ DE FEDERICO, 1976). The continuous transition towards amphibolitized eclogites (AE) is a result of the second Alpine metamorphic overprint under albite-epidote-amphibolite facies conditions. The transformation of (E) to (AE) largely preserved the eo-Alpine textures, which in turn had pseudomorphosed those of the igneous protoliths. The mineralogy of the Sierra Nevada (E) and (AE) is similar to that of other eclogitic rocks from Tethyan ophiolitic complexes (DIETRICH et al., 1974; CORTESOGNO et al., 1977; DAL PIAZ and ERNST, 1978; MESSIGA et al., 1983; POGNANTE, 1985).

The (AOF), which differ from the previous rock types in the absence of garnet, are scarce, and rarer still are the (AGG), characterized by the absence of omphacite. The absence of garnet or omphacite in these rocks is due to the chemical peculiarities of their protoliths.

3. Bulk rock chemistry

Thirty-two representative samples (Table 1) were chosen for geochemical study. Major elements, excluding Na_2O and MgO , and trace elements were determined by XRF following the procedure described by FRANZINI et al. (1972, 1975) and LEONI and SAITTA (1976). Na_2O and MgO were determined by A.A. spectrometry and the loss of ignition at 1000°C by gravimetry. The results are set out in Tables 1 and 2, and plotted in Figs. 3 to 8 along with some analyses already published by BODINIER et al. (1987). The samples are basaltic in composition: the SiO_2 contents range from 45.5% to 50.3% wt. (average 48.32% wt, $\sigma=1.10$) and the FeO^*/MgO ratios range from 1.02 to 3.0. A noticeable scattering of the alkali contents can also be observed, i.e., with Na_2O varying from 3% up to 8% wt. These Na_2O -rich metabasites are enriched in Li (up to 120 ppm) and depleted in K_2O , Rb, Ba and Cu, as a consequence of the sea-floor meta-

morphism that affected these rocks before the Alpine metamorphic events (BODINIER et al., 1987). The K_2O content is very low in all the samples, as may be expected in oceanic basalts.

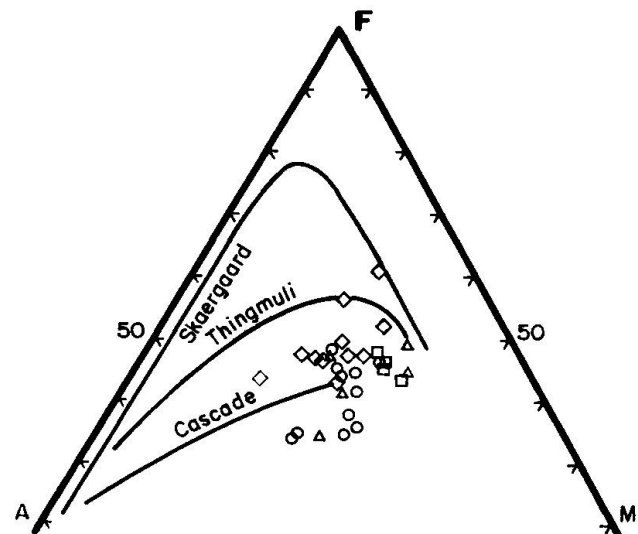


Fig. 3a AFM diagram for the Sierra Nevada metabasites. Symbols corresponding to outcrops: \diamond = Camarate; Δ = Cauchiles; \circ = Puntal de la Caldera; \square = Soportujar.

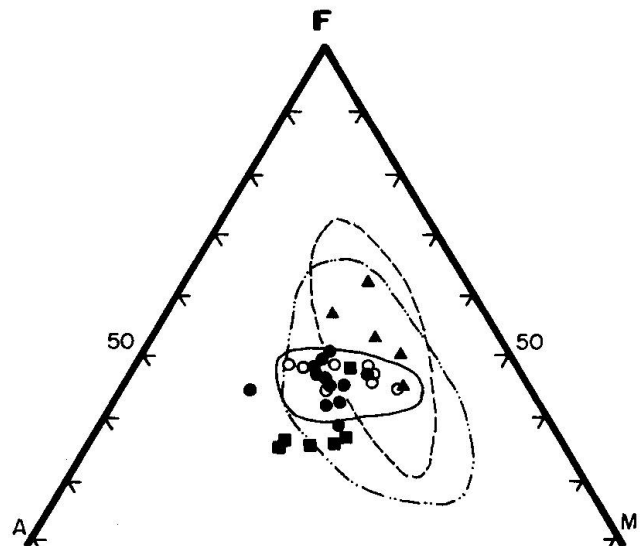


Fig. 3b AFM diagram for the different lithotypes of the Sierra Nevada eclogites and related rocks. Symbols: \bullet = amphibole eclogite; \circ = amphibolitized eclogite; \blacksquare = amphibolitized omphacite felse; \blacktriangle = garnet glaucophanite. The areas encircled by dashed, dotted and solid lines represent the compositional range of the Piemonte Ophiolite Nappe metabasites (DAL PIAZ and ERNST, 1978), of the Gruppo di Volti eclogites (CORTESOGNO et al., 1977) and the M.A.R. basalts drilled at 45°N (WOOD et al., 1979), respectively.

Major element, normative composition and Mg number of the analyzed rocks.

| Big 9: TDF-300 TDF-319 TDF-321 TDF-313 TDF-308 TDF-320 TDF-318 TDF-302 TDF-315 TDF-316 | | | | | | | | | | | |
|--|--------|-------|-------|--------|--------|-------|--------|--------|--------|--------|--------|
| EC-15A | | C-1 | | C-2 | | U-257 | | U-222 | | U-259 | |
| H | | EU-10 | | U-240 | | EU-10 | | U-240 | | EU-10 | |
| 46.61 | 47.74 | 47.74 | 48.73 | 48.62 | 47.07 | 47.14 | 48.48 | 48.93 | 47.07 | 49.12 | 47.16 |
| 48.34 | 48.85 | 49.33 | 45.50 | 47.63 | 48.87 | 50.32 | 48.67 | 45.28 | 50.01 | 46.38 | 49.51 |
| 2.33 | 2.16 | 2.38 | 1.40 | 3.01 | 2.13 | 3.06 | 3.56 | 1.23 | 3.36 | 2.35 | 2.28 |
| 16.82 | 14.47 | 15.04 | 16.87 | 15.84 | 14.79 | 15.35 | 15.65 | 15.49 | 15.73 | 15.24 | 14.18 |
| 10.65 | 11.77 | 12.43 | 15.84 | 11.14 | 12.39 | 10.73 | 11.96 | 20.01 | 10.19 | 12.71 | 10.38 |
| 0.14 | 0.17 | 0.15 | 0.10 | 0.21 | 0.16 | 0.14 | 0.08 | 0.07 | 0.08 | 0.14 | 0.15 |
| 6.19 | 6.86 | 6.40 | 8.42 | 5.17 | 5.94 | 4.79 | 4.89 | 7.60 | 3.69 | 9.88 | 6.80 |
| 7.10 | 8.78 | 5.73 | 4.34 | 9.29 | 8.50 | 7.18 | 6.24 | 4.13 | 6.87 | 6.49 | 7.01 |
| 4.84 | 4.92 | 5.50 | 4.33 | 5.85 | 5.00 | 5.80 | 6.75 | 3.37 | 6.80 | 4.26 | 6.00 |
| 1.15 | 0.23 | 0.18 | 0.25 | 0.13 | 0.47 | 0.14 | 0.24 | 0.25 | 1.19 | 0.26 | 0.35 |
| 0.42 | 0.36 | 0.69 | 0.10 | 0.54 | 0.35 | 0.47 | 0.61 | 0.12 | 0.76 | 0.15 | 0.11 |
| 2.57 | 1.44 | 1.96 | 2.84 | 1.36 | 1.50 | 2.01 | 2.00 | 2.97 | 1.34 | 1.91 | 2.23 |
| 100.55 | 100.01 | 99.99 | 99.99 | 100.17 | 100.00 | 99.99 | 100.65 | 100.52 | 100.02 | 100.00 | 100.00 |
| Total: | | | | | | | | | | | |
| 7.04 | 1.39 | 1.09 | 1.54 | 0.79 | 2.87 | 0.55 | 1.46 | 1.56 | 7.19 | 1.58 | 1.78 |
| 37.12 | 36.93 | 47.88 | 38.22 | 35.95 | 37.98 | 50.68 | 47.10 | 30.14 | 42.79 | 35.37 | 34.31 |
| 21.47 | 17.10 | 16.24 | 21.78 | 17.00 | 17.09 | 15.94 | 12.01 | 20.63 | 9.09 | 22.32 | 20.99 |
| 2.82 | 3.06 | 1.71 | - | 8.02 | 3.12 | - | 6.25 | - | 8.70 | 0.93 | 11.40 |
| 9.46 | 20.18 | 6.71 | - | 20.87 | 19.50 | 13.84 | 12.05 | - | 16.01 | 7.84 | 12.92 |
| 10.71 | 10.86 | 11.72 | 26.26 | 3.47 | 8.97 | 4.29 | 5.11 | 15.26 | 1.39 | 21.27 | 6.22 |
| 5.74 | 5.43 | 6.09 | 4.39 | 6.70 | 5.44 | 6.83 | 7.53 | 4.18 | 4.81 | 5.74 | 4.87 |
| - | - | - | - | - | - | - | - | - | - | 1.65 | 0.06 |
| 4.57 | 4.20 | 5.04 | 2.77 | 5.86 | 4.18 | 6.00 | 6.94 | 2.47 | 6.53 | 4.59 | 4.47 |
| 1.01 | 0.86 | 1.65 | 0.24 | 1.29 | 0.84 | 1.13 | 1.46 | 0.29 | 1.81 | 0.36 | 0.67 |
| 0.07 | - | - | - | 0.05 | - | - | 0.09 | 0.07 | 0.05 | - | 0.98 |
| 64 | 60 | 60 | 48 | 46 | 45 | 51 | 50 | 48 | 46 | 51 | 51 |
| 57 | 57 | 54 | 51 | 51 | 51 | 50 | 48 | 46 | 45 | 51 | 51 |
| 57 | 57 | 54 | 51 | 51 | 51 | 50 | 48 | 46 | 45 | 51 | 51 |
| 58 | 58 | 56 | 56 | 55 | 55 | 55 | 56 | 56 | 56 | 51 | 51 |

[$\text{Mn}/(\text{Mn}+\text{Fe2t})$] with Fe2t standardized to $\text{Fe3t}/\text{Fe2t} = 0.15$

Tab. 2 Chemical averages of the lithotypes from the Sierra Nevada metabasites and MAR basalts.

| | E (x=13) | r | AE (x=9) | r | AOF (x=5) | r | AGG (x=4) | r | MAR (x=12) | r |
|--------------------------------|-------------|-------|-------------|--------|--------------|--------|--------------|--------|---------------|--------|
| SiO ₂ | 48.21 | 0.91 | 48.70 | 1.02 | 48.63 | 0.59 | 46.78 | 2.06 | 49.06 | 0.81 |
| TiO ₂ | 2.34 | 0.78 | 2.37 | 0.90 | 1.90 | 0.47 | 1.77 | 0.54 | 1.73 | 0.89 |
| Al ₂ O ₃ | 16.32 | 1.15 | 15.38 | 1.01 | 16.84 | 1.52 | 15.51 | 1.02 | 14.79 | 1.44 |
| FeO/100 | 10.75 | 0.84 | 11.52 | 0.95 | 9.54 | 1.53 | 14.99 | 3.82 | 11.55 | 2.34 |
| MnO | 0.16 | 0.04 | 0.13 | 0.03 | 0.13 | 0.05 | 0.11 | 0.03 | 0.17 | 0.03 |
| MgO | 6.00 | 0.90 | 6.44 | 1.44 | 6.79 | 0.48 | 8.37 | 1.08 | 7.97 | 2.40 |
| CaO | 8.53 | 0.78 | 8.12 | 1.72 | 7.86 | 0.89 | 6.11 | 2.48 | 11.10 | 0.86 |
| Na ₂ O | 5.42 | 0.83 | 4.83 | 1.01 | 6.17 | 1.18 | 3.74 | 0.66 | 2.50 | 0.53 |
| K ₂ O | 0.45 | 0.38 | 0.31 | 0.33 | 0.31 | 0.08 | 0.23 | 0.04 | 0.40 | 0.46 |
| P ₂ O ₅ | 0.38 | 0.17 | 0.40 | 0.21 | 0.27 | 0.12 | 0.16 | 0.07 | 0.23 | 0.10 |
| L.I. | 1.70 | 0.50 | 1.91 | 0.39 | 1.72 | 0.32 | 2.25 | 0.81 | 1.22 | 0.50 |
| Li | 34.67 | 22.75 | 37.00 | 9.90 | 45.50 | 30.41 | 23.00 | * | - | - |
| Rb | 6.44 | 5.50 | 5.29 | 1.25 | 4.50 | 2.38 | 5.33 | 2.08 | 8.97 | 12.73 |
| Sr | 236.60 | 67.67 | 276.71 | 106.12 | 230.60 | 117.53 | 334.67 | 310.99 | 210.30 | 120.35 |
| Ba | 69.60 | 62.95 | 15.00 | 7.07 | 15.00 | 0.00 | 10.00 | * | 117.33 | 117.53 |
| Sc | 30.97 | 3.56 | 31.35 | 0.50 | 31.65 | 11.24 | 37.30 | * | 38.07 | 6.27 |
| V | 269.80 | 61.13 | 280.86 | 59.04 | 257.20 | 41.25 | 237.33 | 57.71 | 330.50 | 93.75 |
| Cr | 161.60 | 56.87 | 358.57 | 421.76 | 197.40 | 63.24 | 216.67 | 46.69 | 247.44 | 153.33 |
| Co | 30.50 | 5.97 | 38.14 | 9.58 | 27.20 | 9.28 | 36.33 | 3.79 | 47.98 | 7.56 |
| Ni | 62.90 | 18.98 | 81.00 | 46.91 | 79.00 | 24.42 | 93.00 | 55.02 | 146.47 | 87.09 |
| Cu | 9.67 | 2.89 | 24.00 | 21.21 | 11.50 | 6.36 | 9.00 | * | - | - |
| Zn | 91.33 | 56.72 | 121.00 | 86.27 | 72.50 | 10.61 | 28.00 | * | 81.33 | 20.53 |
| La | 12.00 | 9.43 | 13.90 | 14.14 | 19.35 | 8.41 | 10.20 | * | 12.69 | 11.65 |
| Ce | 26.90 | 22.92 | 32.00 | 31.11 | 45.30 | 19.52 | 24.20 | * | 26.47 | 18.92 |
| Nd | 29.65 | 7.43 | 22.55 | 20.86 | 29.60 | 12.73 | 18.00 | * | 15.96 | 8.85 |
| Sm | 4.71 | 3.80 | 5.47 | 4.33 | 6.33 | 2.26 | 5.15 | * | 4.43 | 2.16 |
| Eu | 1.43 | 1.10 | 1.77 | 1.22 | 1.85 | 0.56 | 1.77 | * | 1.51 | 0.65 |
| Tb | 0.84 | 0.46 | 1.04 | 0.60 | 1.06 | 0.28 | 1.01 | * | 0.81 | 0.33 |
| Yb | 3.60 | 0.53 | 3.44 | 1.93 | 2.63 | 0.40 | 2.88 | * | 2.82 | 0.88 |
| Lu | 0.55 | 0.08 | 0.74 | 0.01 | 0.40 | 0.05 | 0.44 | * | 0.46 | 0.15 |
| Y | 33.90 | 4.91 | 33.29 | 7.23 | 42.40 | 28.72 | 27.00 | 3.00 | 32.89 | 11.27 |
| Hf | 4.38 | 1.45 | 4.38 | 3.56 | 3.99 | 0.50 | 3.51 | * | 2.99 | 1.62 |
| Zr | 180.50 | 46.40 | 181.00 | 88.06 | 129.20 | 31.12 | 132.33 | 34.20 | 125.91 | 70.10 |
| Nb | 14.70 | 4.08 | 12.57 | 11.65 | 14.00 | 7.48 | 13.00 | 8.89 | 25.01 | 21.46 |
| Th | 0.98 | 0.66 | 1.09 | 1.17 | 1.58 | 0.17 | 0.46 | * | 1.49 | 1.65 |

Major elements in wt %, minor elements in ppm.

E= Eclogites ; AE= Amphibolitized eclogites ; AOF= Amphibolitized omphacite felses

AGG= Amphibolitized garnet glauconianites ; MAR= Mid-Atlantic Ridge basalts at 36°, 45° and 63° N. r= standard deviation. *= only one analysis.

Table 2 shows the average chemical characteristics of the various lithotypes of the Sierra Nevada metabasites, which may explain their mineralogical differences.

The Sierra Nevada metabasites plot near the centre of the AFM diagram, as do the majority of Alpine ophiolitic eclogites and the P-type M.A.R. basalts (Fig. 3a, b), and they do not follow any obvious trend. Some samples from Camarate and Cauchiles are rich in iron and follow a tholeiitic trend. The Puntal de la Caldera samples plot between the tholeiitic and either the alkaline-sodic or else the calc-alkaline series (Fig. 3a). FeO vs FeO/MgO (Fig. 4) shows the tholeiitic character of the Sierra Nevada metabasites and the iron enrichment of the (AGG). The

(E) and (AE) groups have an intermediate FeO*/MgO ratio while the (AOF) has the lowest value (with one exception) and the (AGG) has the highest value for this ratio. Within the tholeiitic series the (AOF) may correspond to less differentiated magmas, similar to some of the Voltri Mg-metagabbros (MESSIGA et al., 1983) and to the intermediate gabbros of the ophiolitic complexes of the northern Apennines (BECCALUVA et al., 1980; SERRI, 1980). The (AGG) may correspond to more differentiated magmas, similar to the iron-rich gabbro types of these complexes (MOTTANA and BOCCIO, 1975).

The correlation of elements such as HREE, Y, Ti, Zr and Nb indicates that they have not been significantly mobilized during the petrogenetic history of these metabasites (BODINIER et al., 1987) and can be used for their characterization. The Nb/Y vs Zr/TiO₂ diagram (WINCHESTER and FLOYD (1977), Fig. 5, shows that the samples have basaltic and andesite-basaltic compositions with a subalkaline affinity transitional to alkaline sodic. The Nb/Y ratios range from 0.10 to 0.96 (average 0.42, $\sigma = 0.23$). If the Y/Nb ratio is taken as an index of alkalinity (PEARCE and CANN, 1973), all the samples are subalkaline (Y/Nb ratios range from 1.04 to 10.3, average 3.58, $\sigma = 2.75$). The transition elements such as Ti, Cr and Ni indicate a tholeiitic fractionation trend, i.e. an increase in the Ti/Cr ratio with a

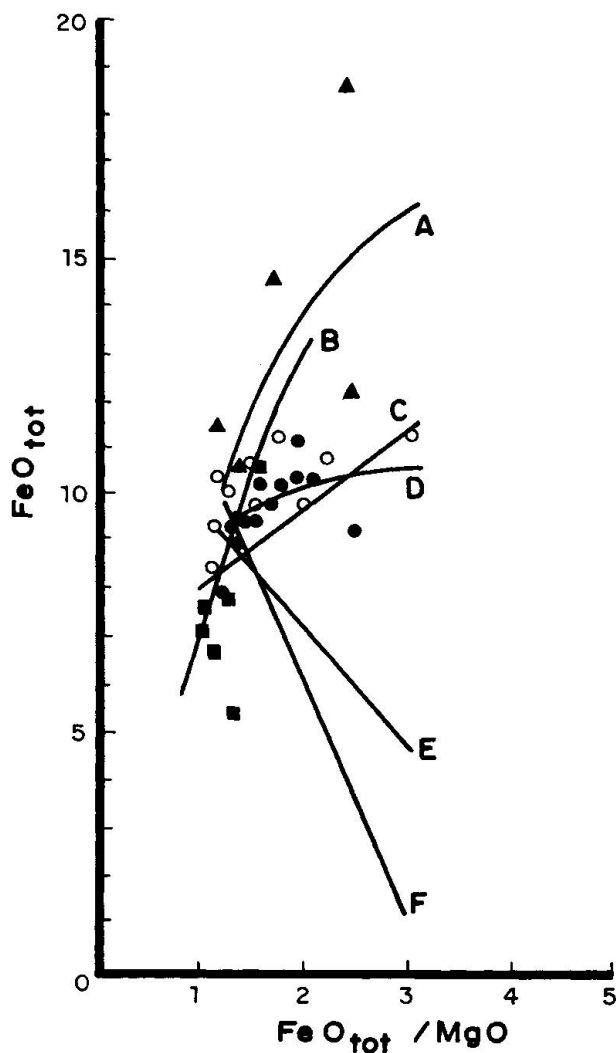


Fig. 4 FeO* versus FeO*/MgO for the Sierra Nevada eclogites and related rocks. Symbols as in Fig. 3b. Fractionation trends for Skærgaard magma (A), abyssal tholeiites (B), island-arc tholeiite series (C,D) and calc-alkaline series (E,F) in MIYASHIRO (1973).

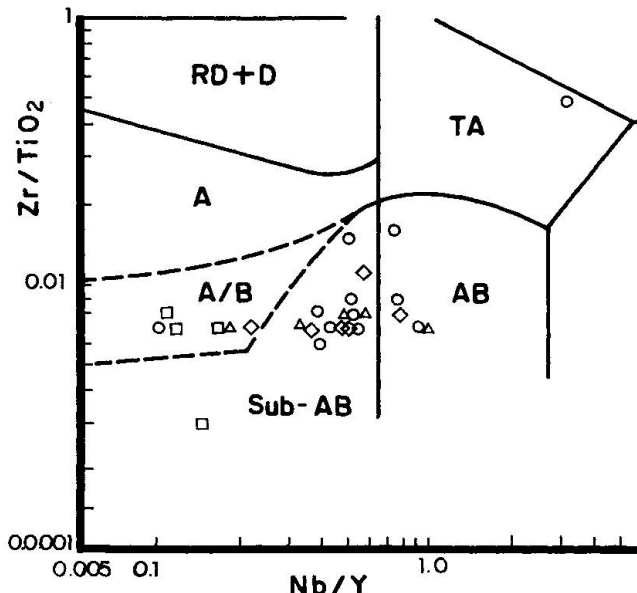


Fig. 5 Nb/Y versus Zr/TiO₂ classificative diagram (WINCHESTER and FLOYD, 1977). Symbols as in Fig. 3a. Sub-AB = subalkaline basalt, AB = alkaline basalt; A/B = basaltic andesite; A = andesite, TA = trachianandesite; RD+D = rhyodacite and dacite.

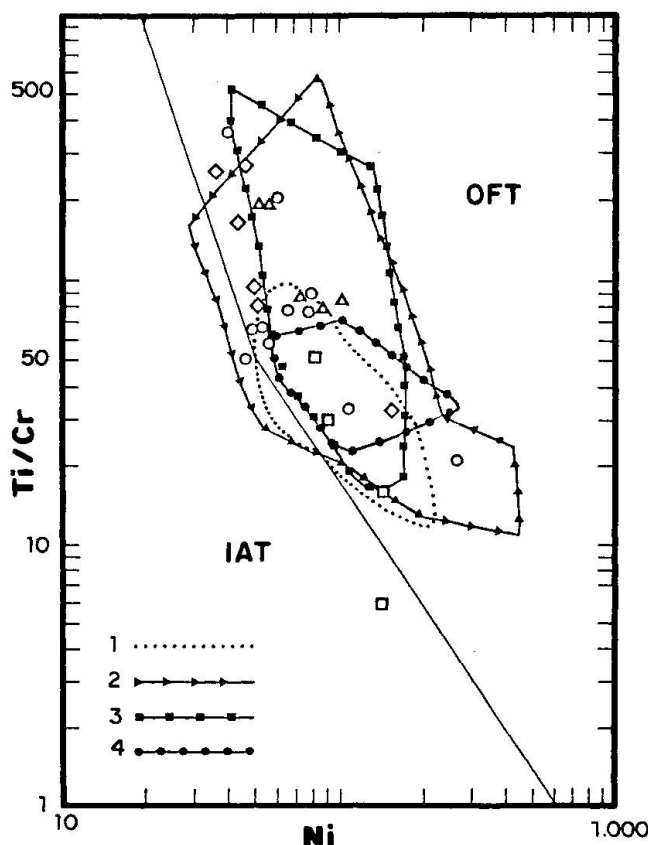


Fig. 6 Ti/Cr versus Ni discriminative diagram between ocean-floor (OFT) and island-arc (IAT) tholeiites (BECCALUVA et al., 1979). Symbols as in Fig. 3a. Fields 1, 2, 3 and 4 represent the variations of the Tethyan ophiolite basaltic rocks from the northern Apennines, Alps, Calabria and Corsica respectively (BECCALUVA et al., 1980).

decrease in the Ni content (Fig. 6). The rocks also plot in the OFT (Ocean-floor tholeiites) field of this diagram (BECCALUVA et al., 1979) as do other western-Tethyan ophiolitic rocks. Likewise they plot, with one exception, in field D (ocean-floor basalts) of the Ti vs Zr diagram (Fig. 7a) (PEARCE and CANN, 1973) or on the continuation of it. Fig. 7b shows that the Ti vs Zr field of the different lithotypes of the Sierra Nevada metabasites overlaps with that of the western Mediterranean ophiolites. The Ti vs V plot (SHERVAIS, 1982) shows that the field of the eclogites matches the MORB field and also that of some ophiolitic rocks from Corsica and the northern Apennines.

Fig. 8 shows the similarity among the patterns of some incompatible and compatible elements of the different types of Sierra Nevada metabasites and that of the average of the basalts from the Mid-Atlantic Ridge at 36°, 45° and 63° N (WOOD et al., 1979), which are also rich in incompatible elements (P-type MORB). The (E)

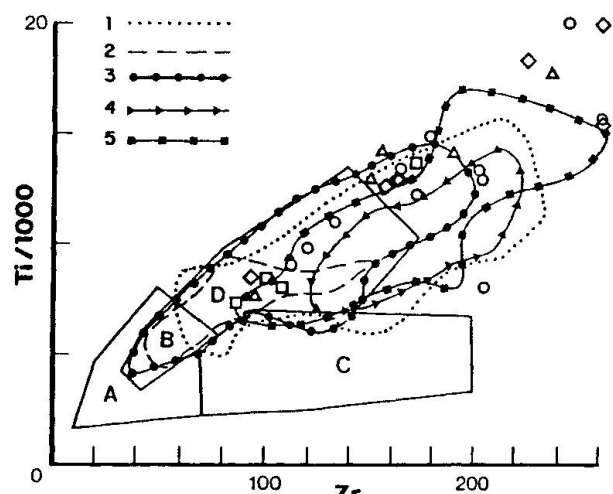


Fig. 7a Ti/1000 versus Zr discriminative diagram (PEARCE and CANN, 1973). Symbols as in Fig. 3a. Fields 1, 2, 3, 4 and 5 represent the variations of the Tethyan ophiolite basaltic rocks, i.e. Voltri praslinite, Monviso metabasalts, northern Apennine basalts and Corsican basalts and metabasalts, respectively (MONVISO, 1980).

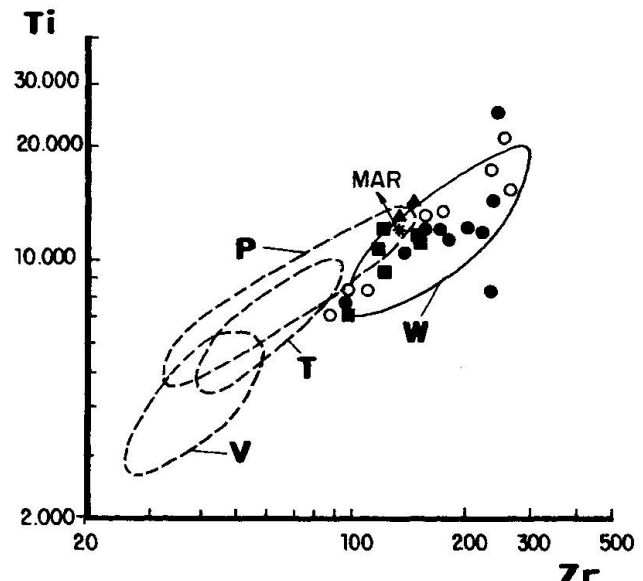


Fig. 7b Ti versus Zr diagram for the Sierra Nevada eclogites and related rocks compared to Mediterranean ophiolitic rocks. Symbols as in Fig. 3b. W = Western Mediterranean ophiolites from Corsica, Eastern Liguria and Engadine (PEARCE, 1980; VENTURELLI et al., 1979, 1981). Eastern Mediterranean ophiolites: P = Pindos, high-Ti lavas (CAPREDI et al., 1980); T = Troodos, Axial sequence (SMEWING and POTTS, 1976); V = Vourinos, Krapa sequence (BECCALUVA et al., 1984).

and the (AE) have similar patterns, while the (AOF) show a higher fractionation of LREE. Furthermore, the (AOF) contain more incompatible trace elements than the (AGG).

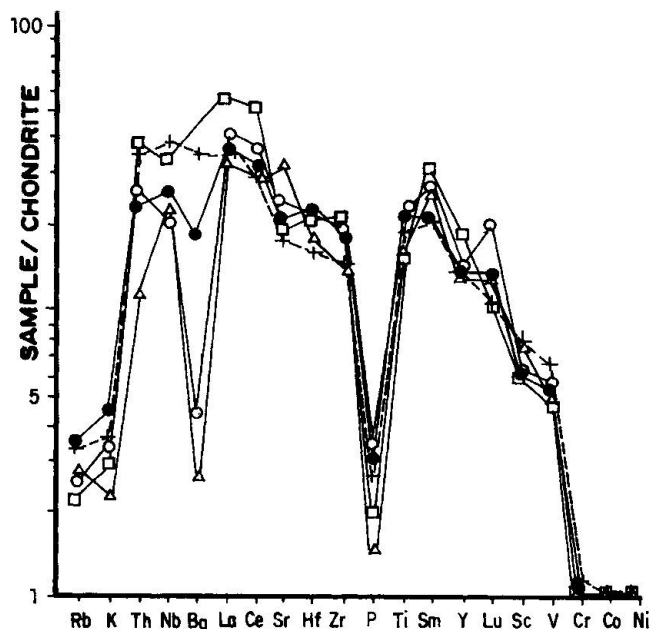


Fig. 8 Chondrite-normalized patterns for the different lithotypes of Sierra Nevada metabasites compared to average values of Mid-Atlantic Ridge basalts at 36°, 45° and 63°N. The elements are arranged approximately in order of increasing bulk-mantle / basaltic-liquid partition coefficient. Chondrite values in Wood et al. (1979). Symbols as in Fig. 3b. + = MAR basalts at 36°, 45° and 63° N. (Wood et al., 1979).

4. Petrography

Semiquantitative modal analyses of the 32 samples are given in Fig. 9. They are grouped according to the different types of metabasites distinguished: (E), (AE), (AOF) and (AGG).

4.1. ECLOGITES (E)

The eclogites are fine- to medium-grained massive rocks. They contain abundant porphyroblasts or microcrystalline aggregates of pink garnets set in a grass-green omphacite matrix. Variable amounts of dark green amphibole, white mica and epidote are also present. Occasional millimetric pseudomorphs of igneous plagioclase may be oriented randomly or slightly subparallelly.

The textures of the primary igneous rocks can still be recognized. Eclogites derived from aphyric basalts have granoblastic or porphyroblastic textures. In the latter case, millimetric poikiloblasts of garnet are set in a nematoblastic matrix of subparallel prisms of symplectite-rimmed omphacite with interstitial amphibole and rutile. The eclogites derived from gabbro or dolerite have metagabbroic, metasubophitic or mylonitic

| | Amphibole Eclogites | | | | | | | | | | Amphibolitized Eclogites | | | | Amphibolitized Omphacite Felses | | | | Garnet Glauconites | | | | | | | | | | | | | |
|----------------|---------------------|---------|---------|-------|---|-------|-------|-------|-------|-------|--------------------------|-----|-----|---------|---------------------------------|-------|---------|-----|--------------------|-------|---------|---------|------|-------|------|------|---------|-----|---------|---------|-------|--------|
| | TDF-308 | TDF-316 | TDF-320 | U-222 | H | EU-10 | U-255 | U-258 | U-259 | U-260 | SN-7A | C-2 | C-3 | TDF-300 | TDF-307 | ES-11 | TDF-318 | S-1 | S-2 | ES-10 | TDF-302 | TDF-321 | SN-8 | U-257 | SN-7 | SN-9 | TDF-319 | C-1 | TDF-313 | TDF-345 | EC-16 | EC-15A |
| GARNET | ■ | ■ | ■ | ● | ● | ● | ● | ● | ● | ● | ● | ● | ● | ● | ● | ● | ● | ● | ● | ● | ● | ● | ● | ● | ● | ● | ● | ● | ● | | | |
| OMPHACITE | ■ | ■ | ■ | ■ | ■ | ■ | ■ | ■ | ■ | ■ | ■ | ■ | ■ | ■ | ■ | ■ | ■ | ■ | ■ | ■ | ■ | ■ | ■ | ■ | ■ | ■ | ■ | ■ | ■ | ■ | | |
| RUTILE | ● | ● | ● | ○ | ○ | ○ | ○ | ○ | ○ | ○ | ○ | ○ | ○ | ○ | ○ | ○ | ○ | ○ | ○ | ○ | ○ | ○ | ○ | ○ | ○ | ○ | ○ | ○ | ○ | ○ | | |
| GLAUCOPHANE | | | | □ | □ | ○ | ○ | ○ | ○ | ○ | ○ | ○ | ○ | ○ | ○ | ○ | ○ | ○ | ○ | ○ | ○ | ○ | ○ | ○ | ○ | ○ | ○ | ○ | ○ | ○ | | |
| KYANITE | | | | | | | | | | | | | | | | | | | | | | | | | | | | | | | | |
| HUMITE | | | | | | | | | | | | | | | | | | | | | | | | | | | | | | | | |
| WHITE MICA | ○ | ○ | ● | ○ | ● | ● | ● | ○ | ○ | ○ | ○ | ○ | ○ | ○ | ○ | ○ | ○ | ○ | ○ | ○ | ○ | ○ | ○ | ○ | ○ | ○ | ○ | ○ | ○ | ● | | |
| HASTINGITE | | | | | | | | | | | | | | | | | | | | | | | | | | | | | | | | |
| Mg-KATAPHORITE | ○ | ○ | ○ | ● | ○ | ○ | ● | ● | ● | ● | ● | ● | ● | ● | ● | ● | ● | ● | ● | ● | ● | ● | ● | ● | ● | ● | ● | ● | ● | ● | | |
| BARROISITE | ○ | ○ | ○ | ● | ○ | ○ | ● | ● | ● | ● | ● | ● | ● | ● | ● | ● | ● | ● | ● | ● | ● | ● | ● | ● | ● | ● | ● | ● | ● | ● | | |
| SYMPLECTITE | ○ | ○ | ○ | ○ | ○ | ○ | ○ | ○ | ○ | ○ | ○ | ○ | ○ | ○ | ○ | ○ | ○ | ○ | ○ | ○ | ○ | ○ | ○ | ○ | ○ | ○ | ○ | ○ | ○ | ○ | | |
| EPIDOTE | | | | | | | | | | | | | | | | | | | | | | | | | | | | | | | | |
| ALBITE | | | | | | | | | | | | | | | | | | | | | | | | | | | | | | | | |
| QUARTZ | | | | | | | | | | | | | | | | | | | | | | | | | | | | | | | | |
| SPHENE | | | | | | | | | | | | | | | | | | | | | | | | | | | | | | | | |
| OPAQUES | | | | | | | | | | | | | | | | | | | | | | | | | | | | | | | | |
| CHLORITE | | | | | | | | | | | | | | | | | | | | | | | | | | | | | | | | |
| BIOTITE | ○ | ○ | | | | | | | | | | | | | | | | | | | | | | | | | | | | | | |

Fig. 9 Metamorphic assemblages and modal contents of the Sierra Nevada eclogites and related rocks. Provenance of the samples: TDF = Camarate; U, H, EU and SN = Puntal de la Caldera; C and EC = Cauchiles; S and ES = Sopotujar.

textures. Narrow (1 to 2 mm thick) continuous or discontinuous garnet coronas have developed at the olivine-plagioclase interface. Igneous pyroxenes are pseudomorphosed by large omphacite crystals speckled with rutile (omphacite 1). These omphacite 1 porphyroblasts are often fragmented and mantled by omphacite 2, without rutile. Omphacite 2 was also formed in the matrix of the (E) surrounded by glaucophane.

Omphacite, almandine, rutile, glaucophane, paragonite and clinzoisite grew during the high P eo-Alpine metamorphic event. Kyanite, clinohumite and probably lawsonite were rare. Omphacite 1 and 2 were partly transformed into an albite-barroisite symplectite during the Alpine s.s. event.

4.2. AMPHIBOLITIZED ECLOGITES (AE)

The eclogites were either partially or wholly transformed to (AE) as a result of prograde metamorphism under albite-epidote-amphibolite-facies conditions during the second Alpine event. The characteristic phases of this event are: barroisite, albit amphibolite-facies conditions during the second Alpine event. The characteristic phases of this event are: barroisite, albite, pistacite and, locally, Mg-kataphorite, sphene and phengite. Some of these Alpine minerals overgrew eo-Alpine ones, i.e. barroisite rims glaucophane and pistacite rims both clinzoisite and paragonite. Partial or total replacement of garnet by barroisite-epidote-albite-ore-phyllosilicate assemblages is a common feature of these rocks.

The metamorphic textures of the (AE) sometimes superimpose a primary subophitic or gabbroic texture, but more usually they are schistose, layered, or even microfolded. Diablastic, poikiloblastic and/or nematoblastic textures may also be found in the same samples.

4.3. AMPHIBOLITIZED OMPHACITE FELSES (AOF)

The (AOF) have textures suggesting various types of protoliths, none of which contained olivine. The metamorphic textures of the most common precursor rocks, pyroxene gabbro and dolerite, are blasto-subophitic to granoblastic. Blastoporphyrhic textures are characteristic of former dikes and sills with plagioclase phenocrysts of up to 2 cm long. These were pseudomorphosed by albite, epidote, paragonitic sericite and subordinate barroisite. The plagioclase

pseudomorphs account for up to 40% vol. of the rock, and are set in a light- to dark-green matrix of symplectitized omphacite and barroisitic amphibole. In some (AOF) samples the pseudomorphosed plagioclase phenocrysts retain their euhedral shape, but usually they are flattened in accordance with the second Alpine schistosity, or even tightly folded. The matrix of the (AOF) consists mainly of albite-amphibole symplectites derived from omphacite, although subsequent recrystallization within some microdomains has formed diablastic or poikiloblastic textures. The Alpine schistosity is clearly outlined by the preferred orientation of barroisite, epidote and sphene, formed during this stage, and by the re-orientation of the earlier formed pseudomorphs from igneous plagioclase and pyroxene.

4.4. AMPHIBOLITIZED GARNET GLAUCO-PHANITES (AGG)

Relics of igneous minerals are not present in these rocks, except for some rare sericite aggregates, which may represent igneous plagioclase. This suggests that aphyric basalts were the parental igneous rocks. The nematoblastic matrix is microfolded and more or less tectonized. Garnet porphyroblasts are abundant and up to one centimetre in diameter. They are usually hypidiomorphic and contain numerous inclusions of rutile, glaucophane, minor clinzoisite and white mica and, very rarely, clinohumite. Garnet fractures are often filled by hastingsite or barroisite-rimmed glaucophane. The matrix is formed of subparallel barroisite crystals with glaucophane cores and of subordinate white mica and rutile. These minerals outline an axial-plane schistosity of isoclinal folds flattened around the garnet porphyroblasts or porphyroclasts.

The eo-Alpine mineral association of the (AGG) comprises glaucophane, rutile, garnet, paragonite and very rarely clinohumite. Paragonitic sericite and chlorite 1 developed during the retrograde stage of this event. Barroisite (occasionally rimming eo-Alpine chlorite 1), epidote, albite, phengite, rutile and ores, which partially replace garnet and glaucophane, represent the Alpine mineral association. Chlorite 2 and green biotite have often developed in the pressure shadows of garnet.

5. Mineral chemistry

The microprobe analyses were carried out at the Central Geological Survey of Prague using an

ARL-SEMQ instrument. Natural minerals were used as standards. Corrections were made following BENCE and ALBEE's procedure (1968). Three samples (SN-7, TDF-300 and TDF-320) were analyzed at the Mineralogisk-Geologisk Museum of Oslo, using an ARL-EMX analyzer fitted with a Link energy-dispersive spectrometer system. In this latter case, spectrum analyses were undertaken by multiple least-square fittings, and standard matrix-correction procedures (ZAF-4) were used. Standards included pure metals, synthetic oxides and natural minerals.

5.1. GARNETS

The garnet values (Tab. 3 and Fig. 10) are averages of 58 analyses from the four localities. Total Fe was calculated as FeO. They are almandine-rich (Alm 52% to 65%) with an average composition of $\text{Alm}_{47}\text{-Pyr}_{20}\text{-Spess}_{3}\text{-Gro}_{29}\text{-And}_1$. The decrease in Ca and increase in Mg at the rims of some zoned garnets suggest that both temperature and pressure were higher during the growth of the rims.

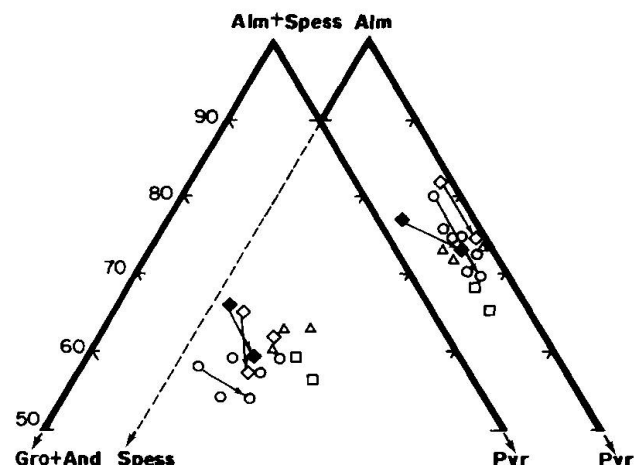


Fig. 10 Plot of chemical composition of garnets in terms of garnet end members, calculated using the method of CAWTHORN and COLLERSON (1974). Symbols as in Fig. 3.a.

Garnets developed only during the eo-Alpine event, as opposed to the assumption of GOMEZ PUGNAIRE and FERNANDEZ SOLER (1987) for other Nevado-Filabrides eclogites. During the

Tab. 3 Average and selected analyses of garnets.

| TDF-320c TDF-320r | | C-2 x=10 | C-3 x=6 | U-222 x=6 | U-255 x=6 | U-258 x=6 | H x=4 | SN-7Ac | SN-7Ar | TDF-300 x=6 | TDF-307c | TDF-307r | S-1 x=3 | S-2 x=3 | EC-15A x=2 | |
|--------------------------------|--------|-------------|------------|--------------|--------------|--------------|----------|--------|--------|----------------|----------|----------|------------|------------|---------------|-------|
| Rock type | E | E | E | E | E | E | E | E | E | AE | AE | AE | AE | AE | AGG | |
| SiO ₂ | 39.00 | 39.20 | 37.84 | 38.51 | 38.18 | 39.95 | 38.68 | 37.98 | 38.21 | 38.42 | 38.38 | 38.83 | 38.48 | 37.76 | 39.36 | 37.80 |
| Al ₂ O ₃ | 21.20 | 21.55 | 21.60 | 21.35 | 22.20 | 21.45 | 21.87 | 22.14 | 21.76 | 21.94 | 21.12 | 22.34 | 22.77 | 21.57 | 22.60 | 21.62 |
| FeO | 26.80 | 26.06 | 27.38 | 27.62 | 25.74 | 23.19 | 26.00 | 25.00 | 27.57 | 25.39 | 27.38 | 29.04 | 26.18 | 26.65 | 23.39 | 28.11 |
| MnO | 2.49 | 0.76 | 1.79 | 1.18 | 1.01 | 1.10 | 1.30 | 1.51 | 0.80 | 0.86 | 0.90 | 0.65 | 0.58 | 1.39 | 1.33 | 0.65 |
| MgO | 3.09 | 4.32 | 4.73 | 5.02 | 4.90 | 3.92 | 5.22 | 3.61 | 3.03 | 5.10 | 4.67 | 3.27 | 4.57 | 5.51 | 5.92 | 5.75 |
| CaO | 7.70 | 8.20 | 6.42 | 6.32 | 8.22 | 9.87 | 7.06 | 9.05 | 10.56 | 9.39 | 6.88 | 7.20 | 8.36 | 6.41 | 5.96 | 5.60 |
| Total | 100.28 | 100.09 | 99.83 | 100.00 | 100.29 | 99.66 | 100.13 | 99.29 | 102.11 | 101.26 | 99.33 | 101.33 | 100.94 | 99.39 | 98.56 | 99.53 |
| Si | 3.078 | 3.067 | 2.978 | 3.020 | 2.970 | 3.135 | 3.015 | 2.998 | 2.956 | 2.958 | 3.032 | 3.028 | 2.975 | 2.970 | 3.090 | 2.967 |
| Al(IV) | - | - | 0.022 | - | 0.030 | - | - | 0.002 | 0.044 | 0.042 | - | - | 0.025 | 0.030 | - | 0.033 |
| Σ | 3.078 | 3.067 | 3.020 | 3.000 | 3.135 | 3.015 | 3.000 | 3.000 | 3.000 | 3.032 | 3.028 | 3.000 | 3.000 | 3.090 | 3.000 | 3.000 |
| Al(VI) | 1.972 | 1.987 | 1.982 | 1.973 | 2.006 | 1.982 | 2.009 | 2.058 | 1.940 | 1.949 | 1.966 | 2.053 | 2.050 | 1.969 | 2.091 | 1.968 |
| Fe ³⁺ | - | - | 0.040 | - | 0.024 | - | - | - | 0.105 | 0.093 | - | - | - | 0.062 | - | - |
| Fe ²⁺ | 1.769 | 1.705 | 1.763 | 1.811 | 1.650 | 1.522 | 1.695 | 1.651 | 1.679 | 1.542 | 1.809 | 1.894 | 1.693 | 1.691 | 1.536 | 1.845 |
| Mn | 0.166 | 0.05 | 0.119 | 0.078 | 0.067 | 0.073 | 0.086 | 0.101 | 0.052 | 0.056 | 0.060 | 0.043 | 0.038 | 0.093 | 0.088 | 0.043 |
| Mg | 0.364 | 0.504 | 0.535 | 0.587 | 0.568 | 0.458 | 0.606 | 0.425 | 0.349 | 0.585 | 0.550 | 0.380 | 0.527 | 0.646 | 0.693 | 0.673 |
| Ca | 0.651 | 0.687 | .541 | 0.531 | 0.685 | 0.830 | 0.590 | 0.765 | 0.875 | 0.775 | 0.582 | 0.602 | 0.693 | 0.540 | 0.501 | 0.471 |
| Σ | 4.992 | 4.933 | 5.000 | 4.980 | 5.000 | 4.865 | 4.985 | 5.000 | 5.000 | 4.968 | 4.972 | 5.000 | 5.000 | 4.910 | 5.000 | |
| Pyr | 12 | 17 | 17 | 19 | 19 | 16 | 20 | 15 | 12 | 20 | 18 | 13 | 18 | 22 | 25 | 22 |
| Sp | 6 | 2 | 4 | 3 | 2 | 2 | 3 | 3 | 2 | 2 | 2 | 1 | 1 | 3 | 3 | 1 |
| Gro | 22 | 23 | 18 | 18 | 22 | 29 | 20 | 26 | 24 | 21 | 20 | 21 | 24 | 15 | 18 | 15 |
| Alm | 60 | 58 | 59 | 60 | 56 | 53 | 57 | 56 | 57 | 52 | 60 | 65 | 57 | 57 | 54 | 62 |
| And | | | | | 2 | 1 | | | 5 | 5 | | | | 3 | | |

Alpine s.s. event garnet was partly replaced by a barroisite-epidote-albite-ore-phyllosilicates association.

5.2. PYROXENES

The chemical composition of 34 pyroxenes is plotted in Fig. 11 and some representative analyses are shown in Table 4. They are omphacites

with jadeite contents ranging from 35% to 50% and an average composition of $\text{Jd}_{44}\text{-}\text{Aug}_{50}\text{-}\text{Ac}_6$. The increase in the jadeite content from the cores towards the rims suggests an increase of pressure from stages A to B (Figs. 14 and 15). This is contrary to the findings of GOMEZ PUGNAIRE and FERNANDEZ SOLER (1987) who have reported omphacite with inverse zonation from the Nevado-Filábride eclogites of the Sierra de Baza.

Tab. 4 Representative analyses of clinopyroxenes.

| | TDF-320 | C-3 | H | U-255 | U-258 | U-222c | U-222r | U-260c | U-260r | SN-7Ac | SN-7Ar | S-2 |
|--------------------------------|---------|-------|-------|-------|--------|--------|--------|--------|--------|--------|--------|-------|
| Rock types | E | E | E | E | E | E | E | E | E | E | E | AE |
| SiO ₂ | 56.02 | 56.74 | 56.28 | 57.54 | 56.82 | 57.34 | 57.35 | 57.08 | 57.94 | 55.74 | 57.94 | 57.46 |
| TiO ₂ | 0.03 | 0.06 | 0.09 | 0.19 | 0.08 | 0.11 | 0.09 | 0.06 | 0.09 | 0.08 | 0.09 | 0.05 |
| Al ₂ O ₃ | 10.60 | 10.07 | 10.46 | 9.89 | 9.70 | 10.47 | 10.36 | 8.16 | 10.62 | 10.14 | 12.18 | 10.39 |
| FeO | 8.22 | 8.45 | 5.78 | 5.37 | 8.77 | 6.01 | 6.65 | 9.80 | 6.98 | 5.89 | 5.50 | 5.87 |
| MnO | 0.04 | 0.07 | - | 0.10 | 0.06 | 0.06 | 0.04 | 0.08 | - | - | - | 0.06 |
| MgO | 6.33 | 6.19 | 8.52 | 8.41 | 7.09 | 8.46 | 7.52 | 7.46 | 7.15 | 7.70 | 6.82 | 7.97 |
| CaO | 10.70 | 10.24 | 11.12 | 12.16 | 10.27 | 11.17 | 10.64 | 10.65 | 10.24 | 13.56 | 10.77 | 11.75 |
| Na ₂ O | 7.03 | 7.37 | 6.55 | 6.05 | 7.55 | 6.73 | 7.09 | 7.41 | 6.54 | 7.30 | 8.06 | 6.17 |
| Total | 98.97 | 99.19 | 98.80 | 99.71 | 100.34 | 100.35 | 100.26 | 100.72 | 100.26 | 100.41 | 99.71 | 99.72 |
| Si | 2.038 | 2.058 | 2.031 | 2.070 | 2.031 | 2.039 | 2.045 | 2.040 | 2.080 | 1.976 | 1.975 | 2.068 |
| Al (IV) | - | - | - | - | - | - | - | - | - | 0.024 | 0.025 | - |
| Σ | 2.038 | 2.058 | 2.031 | 2.070 | 2.031 | 2.039 | 2.045 | 2.040 | 2.080 | 2.000 | 2.000 | 2.068 |
| Al | 0.454 | 0.431 | 0.445 | 0.419 | 0.409 | 0.439 | 0.456 | 0.344 | 0.449 | 0.400 | 0.483 | 0.441 |
| Ti | 0.001 | 0.002 | 0.002 | 0.005 | 0.002 | 0.003 | 0.002 | 0.002 | 0.002 | 0.002 | 0.005 | 0.001 |
| Fe ³⁺ | - | - | - | - | 0.480 | - | - | 0.085 | - | 0.122 | 0.112 | - |
| Fe ²⁺ | 0.250 | 0.256 | 0.174 | 0.162 | 0.214 | 0.179 | 0.198 | 0.208 | 0.210 | 0.053 | 0.050 | 0.177 |
| Mn | 0.001 | 0.002 | - | 0.003 | 0.002 | 0.002 | 0.001 | 0.002 | - | - | - | 0.002 |
| Mg | 0.343 | 0.335 | 0.458 | 0.451 | 0.378 | 0.448 | 0.400 | 0.397 | 0.383 | 0.407 | 0.360 | 0.428 |
| Ca | 0.417 | 0.398 | 0.430 | 0.469 | 0.393 | 0.426 | 0.407 | 0.408 | 0.421 | 0.515 | 0.408 | 0.453 |
| Na | 0.496 | 0.518 | 0.458 | 0.422 | 0.523 | 0.464 | 0.490 | 0.513 | 0.455 | 0.502 | 0.581 | 0.431 |
| Σ | 1.962 | 1.942 | 1.969 | 1.930 | 1.969 | 1.961 | 1.955 | 1.960 | 1.920 | 2.000 | 2.000 | 1.932 |
| Aug | 49.4 | 46.5 | 53.3 | 57.8 | 46.1 | 52.0 | 49.8 | 47.5 | 51.8 | 49.9 | 41.7 | 55.4 |
| CaTs | - | - | - | - | - | - | - | - | - | 0.4 | 0.6 | - |
| Jd | 46.2 | 44.4 | 45.2 | 42.2 | 42.2 | 44.7 | 46.8 | 35.1 | 47.5 | 41.6 | 49.9 | 44.6 |
| Ac | 4.4 | 9.1 | 1.5 | - | 11.7 | 3.3 | 3.5 | 17.3 | 0.72 | 8.1 | 7.8 | - |

5.3. AMPHIBOLES

The chemical composition of 30 amphiboles is plotted in Figs. 12 and 13, and shown in Table 5. The structural formulae and Fe^{3+}/Fe^{2+} proportions were determined by the method of ROBINSON et al. (1982). According to LEAKE (1978) the amphiboles can be classified as glaucophane, barroisite, Mg-kataphorite and actinolite. The glaucophane is the only eo-Alpine amphibole. It is

scarce and generally rimmed by barroisite, which formed during the main Alpine s.s. event along with some Mg-kataphorite and actinolite.

On BROWN's (1977) diagram (Fig. 13) the different Sierra Nevada amphiboles plot into three areas corresponding to different P-T conditions, which may be correlated with different blastesis stages (Figs. 14, 15). The glaucophanes plot with the Shuksan amphiboles, generated at about 7 kbar. The barroisites, Mg-kataphorites and

Tab. 5 Representative analyses of amphiboles.

| | TDF-320 | U-255 | U-260 | C-2 | C-3 | TDF-300 | TDF-307 | S-1 | S-2 | SN-7 | C-1 | EC-15A |
|--------------------------------|---------|--------|-------|-------|-------|---------|---------|-------|-------|-------|-------|--------|
| Rock types | E | E | E | E | E | AE | AE | AE | AE | E | AOF | GG |
| SiO ₂ | 44.53 | 53.42 | 44.58 | 46.52 | 45.15 | 46.71 | 49.13 | 46.98 | 47.53 | 45.43 | 47.90 | 57.54 |
| TiO ₂ | 0.38 | 0.32 | 0.44 | 0.53 | 0.46 | 0.35 | 0.38 | 0.44 | 0.45 | 0.21 | 0.47 | 0.02 |
| Al ₂ O ₃ | 14.34 | 12.35 | 14.47 | 15.99 | 14.67 | 13.66 | 12.62 | 13.95 | 11.30 | 15.92 | 15.12 | 10.85 |
| FeO† | 15.93 | 9.33 | 15.67 | 12.42 | 12.42 | 12.42 | 12.44 | 11.23 | 10.79 | 11.33 | 12.33 | 12.19 |
| MnO | 0.17 | 0.07 | 0.14 | 0.17 | 0.08 | 0.14 | - | 0.09 | 0.09 | 0.12 | 0.11 | - |
| MgO | 9.27 | 12.98 | 9.25 | 10.91 | 11.81 | 11.19 | 11.49 | 12.36 | 14.02 | 10.97 | 10.83 | 9.03 |
| CaO | 7.90 | 7.49 | 6.48 | 6.61 | 6.59 | 6.23 | 6.60 | 7.85 | 8.23 | 7.08 | 6.53 | 1.02 |
| Na ₂ O | 3.83 | 3.97 | 4.34 | 5.27 | 4.95 | 4.59 | 4.72 | 3.45 | 2.95 | 5.34 | 4.72 | 6.75 |
| K ₂ O | 0.66 | 0.32 | 0.40 | 0.44 | 0.48 | 0.41 | 0.26 | 0.55 | 0.38 | 0.71 | 0.52 | 0.01 |
| Total | 97.01 | 100.25 | 95.77 | 98.86 | 96.61 | 95.70 | 97.59 | 96.90 | 95.74 | 97.11 | 98.53 | 97.41 |
| Si | 6.504 | 7.277 | 6.513 | 6.534 | 6.461 | 6.728 | 6.959 | 6.664 | 6.776 | 6.542 | 6.723 | 7.958 |
| Al | 1.496 | 0.723 | 1.487 | 1.466 | 1.539 | 1.272 | 1.041 | 1.336 | 1.224 | 1.458 | 1.277 | 0.042 |
| | 8 | 8 | 8 | 8 | 8 | 8 | 8 | 8 | 8 | 8 | 8 | 8 |
| Al | 0.974 | 1.260 | 1.006 | 1.181 | 0.936 | 1.067 | 1.066 | 0.997 | 0.676 | 1.244 | 1.225 | 1.727 |
| Ti | 0.042 | 0.033 | 0.048 | 0.056 | 0.050 | 0.038 | 0.035 | 0.047 | 0.048 | 0.023 | 0.050 | 0.002 |
| Fe ³⁺ | 0.758 | 0.106 | 1.052 | 0.669 | 1.022 | 0.869 | 0.558 | 0.819 | 1.063 | 0.363 | 0.611 | 0.197 |
| Fe ²⁺ | 1.188 | 0.957 | 0.863 | 0.739 | 0.464 | 0.627 | 0.915 | 0.513 | 0.223 | 1.002 | 0.836 | 1.213 |
| Mg | 2.018 | 2.635 | 2.014 | 2.284 | 2.519 | 2.402 | 2.425 | 2.613 | 2.979 | 2.354 | 2.265 | 1.961 |
| Mn | 0.021 | 0.003 | 0.017 | 0.020 | 0.010 | 0.017 | - | 0.011 | 0.011 | 0.015 | 0.013 | - |
| | 5 | 5 | 5 | 5 | 5 | 5 | 5 | 5 | 5 | 5 | 5 | 5 |
| Ca | 1.236 | 1.093 | 1.014 | 0.995 | 1.010 | 0.961 | 1.002 | 1.193 | 1.257 | 1.092 | 0.952 | 0.151 |
| Na | 0.764 | 0.907 | 0.986 | 1.005 | 0.990 | 1.039 | 0.998 | 0.807 | 0.743 | 0.908 | 1.018 | 1.810 |
| | 2 | 2 | 2 | 2 | 2 | 2 | 2 | 2 | 2 | 2 | 2 | 1.961 |
| Na | 0.321 | 0.142 | 0.244 | 0.430 | 0.384 | 0.243 | 0.298 | 0.136 | 0.073 | 0.583 | 0.266 | - |
| K | 0.123 | 0.056 | 0.075 | 0.079 | 0.088 | 0.075 | 0.047 | 0.096 | 0.058 | 0.130 | 0.093 | 0.002 |
| | 0.444 | 0.197 | 0.319 | 0.509 | 0.471 | 0.319 | 0.345 | 0.232 | 0.131 | 0.713 | 0.360 | 0.002 |

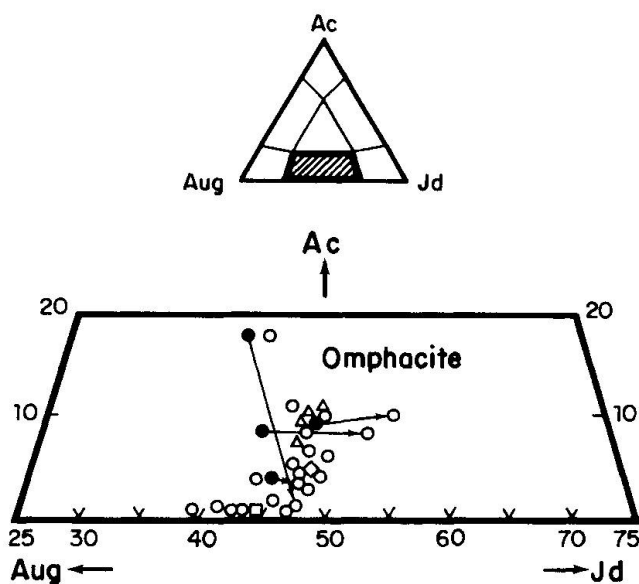


Fig. 11 Aug-Ac-Jd diagram (ESSENE and FYFE, 1967) for the clinopyroxenes from the Sierra Nevada metabasites. Symbols as in Fig. 3a. The arrows connect the cores (solid symbols) with the rim (open symbols) of the zoned pyroxenes.

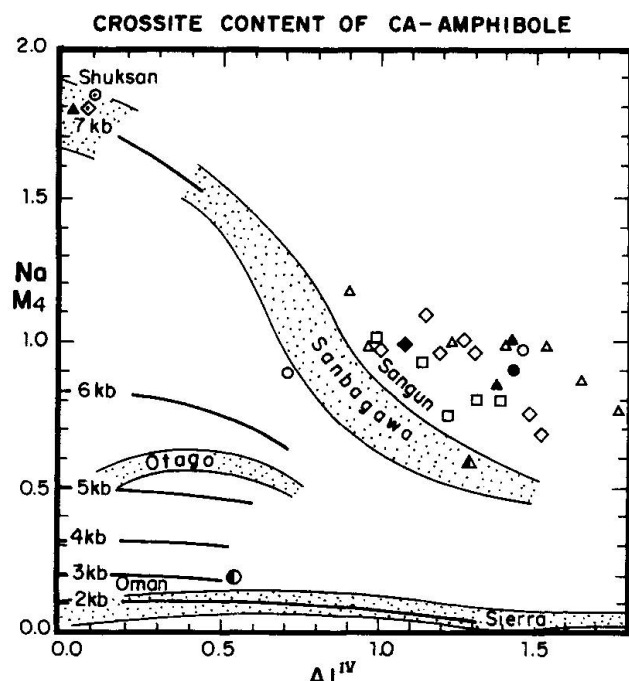


Fig. 13 Plot of the Sierra Nevada metabasite amphiboles on Brown's diagram (1977) showing a tentative estimate of relationships pressure - NaM_4 , and temperature - $\text{Al}(\text{IV})$. Symbols for localities and types of amphiboles as in Fig. 12.

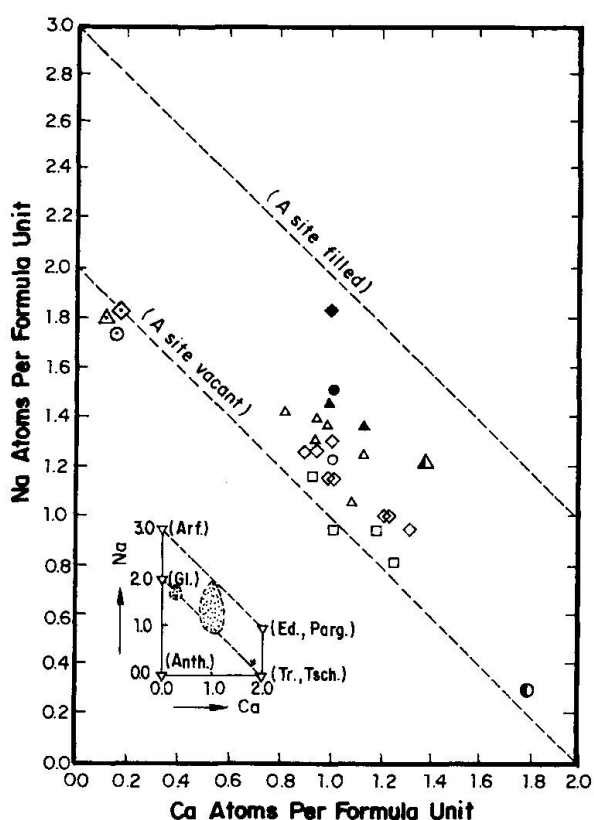


Fig. 12 Proportions of Na and Ca atoms per formula unit in the analyzed amphiboles. Symbols for localities as in Fig. 3a. Symbols containing a dot = glaucophane; solid symbols = Mg-kataphorite; \blacktriangle = hastingsite; \bullet = actinolite.

hastingsites plot above the field of the Sambagawa and Sangun terranes. The somewhat higher $\text{Al}(\text{IV})$ content for the Sierra Nevada Alpine amphiboles would correspond to a formation pressure of about 9 kbar. Finally the actinolites, formed by diaphoresis of the barroisitic amphiboles, plot in an area indicating a pressure of 3 kbar, which would correspond to the final retrograde stage of the Alpine s.s. event.

Other minerals analyzed are (Table 6): eo-Alpine kyanite, filling veins microfolded during the Alpine s.s. event, with a composition close to stoichiometric Al_2SiO_5 ; eo-Alpine paragonite (muscovite 6.9%, margarite 1.6%) rimmed by Alpine s.s. pistacitic epidote; Alpine s.s. albite (anorthite 4%), and green biotite, diaphoretic from garnet, with $\text{Mg}/(\text{Mg}+\text{Fe}) = 0.18$.

6. P-T-t path and metamorphic evolution

Mineral chemistry, microtextural analyses and radiometric ages of the Sierra Nevada eclogites and related rocks record an evolution with five discernible metamorphic stages (Figs. 14 and 15). Stages A, B and C belong to the eo-Alpine metamorphic event, and stages D and E to the Alpine s.s. event. The major eo-Alpine blastesis

Tab. 6 Analyses of kyanite, white mica, biotite, epidote and albite.

| | Kyanite SN-7 | White mica TDF-307 | Biotite TDF-320 | Epidote TDF-307 | Epidote TDF-320 | Albite TDF-307 |
|----------------------------------|-----------------|-----------------------|--------------------|--------------------|--------------------|-------------------|
| Rock types | E | AE | E | AE | E | AE |
| SiO ₂ | 36.74 | 48.37 | 37.10 | 39.26 | 39.25 | 65.54 |
| TiO ₂ | - | 0.19 | 0.53 | - | 0.06 | - |
| Al ₂ O ₃ | 62.02 | 40.00 | 18.70 | 26.68 | 27.10 | 20.23 |
| Fe ₂ O ₃ † | - | - | - | 9.07 | 8.60 | - |
| FeO† | 0.61 | 0.84 | 20.10 | - | - | 0.48 |
| MnO | - | - | 0.53 | 0.11 | 0.03 | - |
| MgO | - | 0.13 | 10.45 | 0.05 | 0.07 | - |
| CaO | - | 0.21 | - | 22.98 | 22.85 | 0.89 |
| Na ₂ O | - | 6.63 | 0.30 | - | - | 11.47 |
| K ₂ O | - | 0.76 | 9.70 | - | - | - |
| Si | 6.054 | 5.539 | 3.229 | 3.223 | 2.924 | - |
| Ti | 0.018 | 0.059 | - | 0.004 | - | - |
| Al (IV) | 1.946 | 2.461 | - | - | 1.064 | - |
| Al (VI) | 3.958 | 0.829 | 2.586 | 2.623 | - | - |
| Fe ³⁺ | - | - | 0.624 | 0.591 | - | - |
| Fe ²⁺ | 0.088 | 2.509 | - | - | 0.018 | - |
| Mn | - | 0.067 | 0.008 | 0.002 | - | - |
| Mg | 0.024 | 2.325 | 0.006 | 0.009 | - | - |
| Ca | 0.028 | - | 2.025 | 2.010 | 0.043 | - |
| Na | 1.609 | 0.087 | - | - | 0.992 | - |
| K | 0.121 | 1.847 | - | - | - | - |
| Para | 91.5% | | Clnz 41.8% | Clnz 44.9% | An 4.1% | |
| Musc | 6.9% | | Pist 57.4% | Pist 54.9% | Ab 95.9% | |
| Marg | 1.6% | | Piem 0.7% | Piem 0.2% | | |

(stages A and B) took place under eclogite-facies conditions, while the Alpine s.s. metamorphic event developed under albite-epidote-amphibolite-facies conditions (stage D). Retrograde stages C and E are not pervasive.

Pressure and temperature estimates of the metamorphic stages of the Sierra Nevada eclogites and related rocks are shown in Figure 15, along with the proposed prograde and retrograde P-T trajectories for both the eo-Alpine and the Alpine metamorphic events. In the Betic Cordilleras the two events correspond to distinct compressive periods, caused by the relative displacement of the Iberian and African plates, resulting in two subduction episodes of the Nevado-Filabride Complex beneath the Alpujarride Complex (PUGA and DIAZ DE FEDERICO, 1976; DIAZ DE FEDERICO et al., 1977; PUGA, 1980). This is similar to the tectonometamorphic evolution in the Alps (i.e., eo-Alpine and Lepontine events, this latter composed in turn by meso- and neo-Alpine). In the Alps, these events were separated by the Paleocene «restoration period» (TRÜMPY, 1973) or «quiescent stage» (DAL PIAZ and ERNST, 1978), during which the compressive regime ceased and was replaced by transcurrent movements. DESMONS (1977) has reported that each climax of the different Alpine metamorphic events (early, middle and late) was followed by a drop in temperature and pressure, with a con-

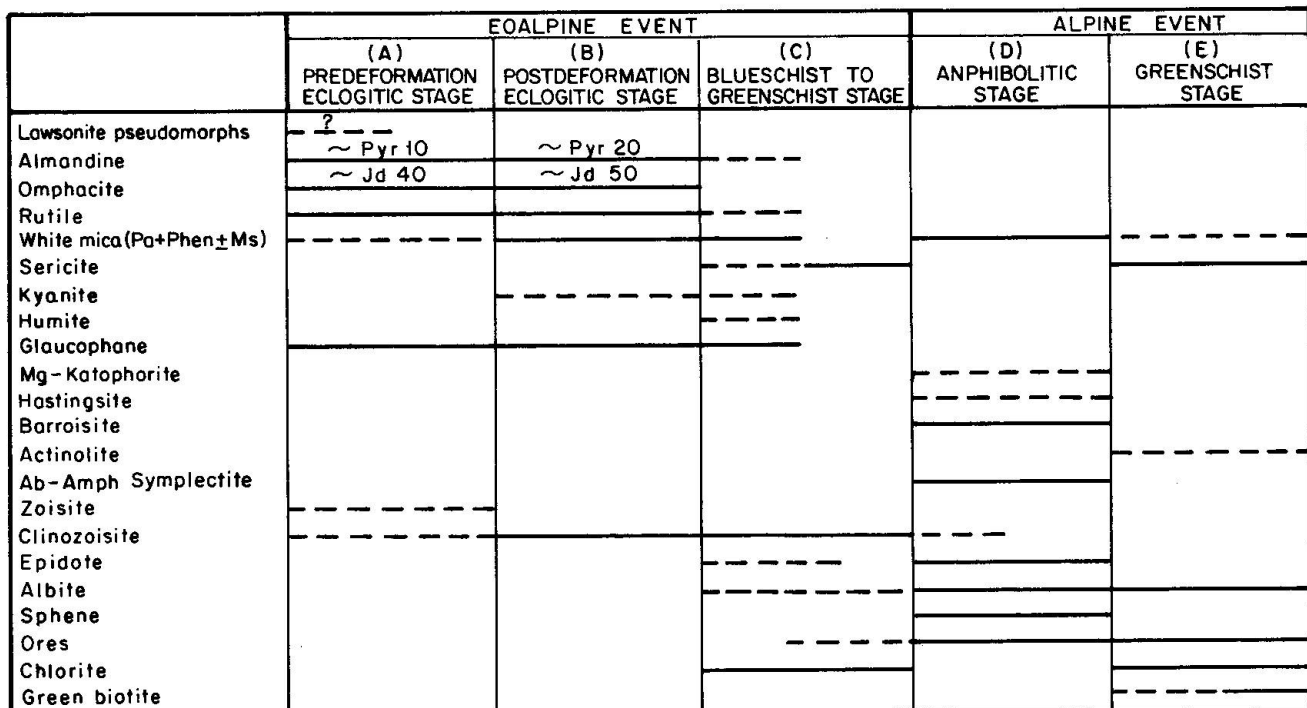


Fig. 14 Schematic diagram showing mineral assemblages and metamorphic stages in the Sierra Nevada eclogites and related rocks. Dashed line indicates occasional occurrence.

comitant retrogression into greenschist-facies metamorphism. This author interpreted the eo-Alpine and meso-Alpine stages as representing two subduction periods. The retrograde metamorphic events in the Sierra Nevada have been interpreted as being due to the buoyant return of part of the material subducted during each of the compressive periods. These retrogressive stages (C and E) are represented in the Sierra Nevada eclogites and related rocks by associations of greenschist facies, although the blastesis of the C stage was partly obliterated during the prograde stage D of the Alpine s.s. event.

6.1. THE EO-ALPINE METAMORPHIC EVENT

Inclusions in the garnets indicate that the prograde PT-path (see Fig. 15) passed through glaucophane-schist-facies conditions previous to eclogitic stage A. The metamorphic climax, stage B, was reached also in eclogitic conditions. During the subsequent exhumation process the path was reversed, passing from eclogite-facies via glaucophane-schist to greenschist-facies conditions (stage C).

During the prograde path towards stage A some hydrous phases, such as epidote, amphibole and probably lawsonite, now included in garnet and omphacite, were formed. This may indicate the previous existence of hydrous igneous phases (such as biotite and/or amphibole), which have indeed been preserved in some less transformed metabasites of the same complex (MORTEN et al., 1987) and probably also an ocean-floor hydration process prior to the subduction (BODINIER et al., 1987). During the restoration process (from B to C stages) eo-Alpine minerals such as kyanite, white mica, glaucophane and clinozoisite appeared in tiny cross-cutting veins or pseudomorphosing the relics of igneous plagioclase. This suggests that the fluid pressure during the formation of the Sierra Nevada eclogites must have been close to the lithostatic pressure. The fluid phase during the eo-Alpine event would have been mainly aqueous with a low CO_2 content. According to HUNT and KERRICK (1977), a 20% CO_2 content would be sufficient to explain the stability of rutile appearing in this event instead of sphene.

Based on the mineral associations and the experimental phase equilibria evidence, the following inferences about the physical conditions that prevailed in each of the successive stages of blastesis can be made.

If lawsonite was formed during the prograde metamorphism, according to the hypothetical

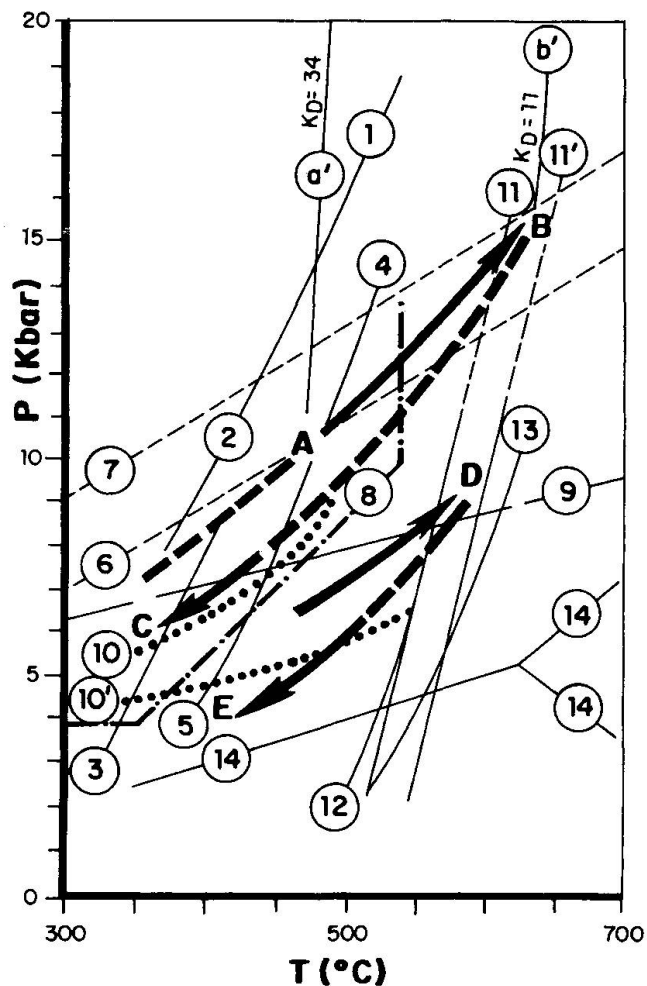


Fig. 15 P-T-t diagram showing the experimentally or calculated equilibrium curves and estimated metamorphic conditions during the formation of the eclogites and related rocks of the Sierra Nevada Complex. Arrows indicate probable prograde and retrograde paths for eo-Alpine and Alpine metamorphic events. A, B and C are successive metamorphic stages of the eo-Alpine event. D and E are the stages of the Alpine s.s. event. Encircled numbers on the curves correspond to the following reactions: 1-2: $\text{Law} + \text{Jd} = \text{Zoi} + \text{Pa} + \text{Q} + \text{H}_2\text{O}$ (HOLLAND, 1979); 3: $5\text{Law} = 2\text{Zoi} + \text{Ma} + 2\text{Q} + 8\text{H}_2\text{O}$ (NITSCH, 1974); 4: $\text{Law} = \text{Zoi} + \text{Ky} + \text{Q} + \text{fluid}$ (NEWTON and KENNEDY, 1963); 5: $\text{Law} = \text{An} + \text{fluid}$ (NEWTON and KENNEDY, 1963); 6: $\text{Ab} + \text{Di} = \text{Omp}(\text{Jd}_{40}) + \text{Q}$ (KUSHIRO, 1969); 7: $\text{Ab} + \text{Di} = \text{Omp}(\text{Jd}_{50}) + \text{Q}$ (KUSHIRO, 1969); 8: Stability field of glaucophane (MARESCH, 1977); 9: $4\text{An} + \text{Ab} + 2\text{H}_2\text{O} = \text{Pa} + 2\text{Zoi} + 2\text{Q}$ (FRANZ and ALTHAUS, 1977); 10-10': Stability field of barroisitic amphibole (ERNST, 1979); 11-11': co-existence field of chloritoid and staurolite (HOSCHEK, 1969); 12: $\text{S} = 6\text{Fo} + \text{T} + 9\text{H}_2\text{O}$ (SCARFE and WYLLIE, 1967); 13: upper stability of antigorite (EVANS et al., 1976); 14: $\text{And} = \text{Ky} = \text{Sill}$ (RICHARDSON et al., 1969). a and b represent the minimum temperature calculated from $K_D(\text{Fe}^{2+}/\text{Mg})$ of the omphacite-garnets pairs, according to the ELLIS and GREEN (1979) thermometer, for the cores at stage A and for the rims at stage B, respectively.

reaction: $\text{An} + \text{fluid} = \text{Law}$, as some sericite-kyanite-zoisite aggregates seem to indicate, then the first reaction which would have taken place in these rocks would have been the breakdown of lawsonite, as shown in curves 2, 3, 4 or 5 (Fig. 15). The absence of lawsonite and the presence of zoisite, kyanite and omphacite (Jd_{40}) (curve 6) indicate a lower pressure limit of about 10 kbar for stage A. The Fe-Mg distribution coefficients between the co-existing garnet and omphacite (KD values = 34) for this minimum pressure indicate a temperature of around 470°C (ELLIS and GREEN, 1979). For stage B, on the other hand, where the omphacite contains up to 50% jadeite, the pressure, according to curve 7, extrapolated to low pressure from the data of KUSHIRO (1969), may have been in the range of 16 kbar or more and the temperature estimate for $\text{KD}=11$ would be 640°C . The estimated temperature and pressure for stage B would conform with the presence of stable antigorite (curves 12 and 13, Fig. 15) and of chloritoid-staurolite assemblages (curves 11 and 11', Fig. 15) in the associated serpentinites and micaschists, respectively.

The textural evidence suggests that glauco-phane, the lower stability limit of which is indicated by curve 8 (MARESCH, 1977), was formed mainly during the retrograde metamorphic period (from B to C stages). Its pressure conditions would be about 7 kbar, according to BROWN's diagram (Fig. 13). Curve 9 shows the conditions under which some of the igneous plagioclases, which may have remained untransformed in the earlier stages (MORTEN et al., 1987), would be replaced via hydration reactions by an association of paragonitic sericite, clinozoisite and quartz.

The K/Ar date of 60 Ma. obtained for white mica of the Caldera Unit of the Sierra Nevada Complex, which underwent the same metamorphic evolution as the ophiolitic nappe, suggests an uplift of the subducted material during the Paleocene (PUGA and DIAZ DE FEDERICO, 1976). If the rapid cooling rate accepted for the Alpine chains $>10^\circ\text{C/Ma}$. (CARPENA et al., 1986) also holds for the Betic Cordilleras, the time span during which the temperature decreased from about 640°C (the maximum attained during stage B) to 350°C (corresponding to the closing of the K/Ar system for the dated white mica) would be somewhat less than 29 Ma. This would place the eo-Alpine metamorphic climax within the Late Cretaceous. The K-Ar dating of an eo-Alpine chloritoid from the San Francisco Unit of the Sierra Nevada Complex, giving 85 ± 4 Ma. (PORTUGAL et al., 1988), points to the same age for this climax. The uplift of a part of the Alpine

Chain during the Upper Cretaceous, after the eclogitic metamorphism, has also been reported by CARPENA et al. (1986) based on radiometric data, and by CHIESA et al. (1977) based on sedimentological evidence. These data correspond well with the model proposed by many authors for the eo-Alpine event in the Alps (HUNZIKER, 1974; BOCQUET et al., 1974; DELALOYE and DEMONS, 1976; CHOPIN and MALUSKI, 1980; HUNZIKER and MARTINOTTI, 1984).

6.2. THE ALPINE S.S. METAMORPHIC EVENT

The eo-Alpine textures and mineral associations were overprinted by those of stages D and E of the Alpine s.s. event (Figs. 14 and 15). The physical conditions during stage D were those of the albite-epidote-amphibolite facies, reaching the limit with the almandine-amphibolite facies at the metamorphic climax (Fig. 15). In the amphibolitic stage D the pre-existing eclogitic minerals and those formed during the retrogressive stage C were replaced to variable extents by an association of barroisite-epidote-albite. The retrograde metamorphic path terminated at stage E under greenschist-facies conditions.

The replacement of omphacite and garnet by hydrous phases, mainly amphibole, epidote and phyllosilicates, and the formation of numerous tiny veins of barroisite, actinolite, pistacite, albite and chlorite indicate that the water pressure increased during this event. The development of magnetite and hematite during stages D and E, and the presence of sphene instead of rutile during stage D, both indicate that the fluid phase must have been richer in water than during the eo-Alpine event. Despite the high fluid pressure deduced for the metamorphic process, there appears to have been no bulk-rock metasomatism at the amphibolitic stage, except for a slight increase in H_2O and in the $\text{Fe}_2\text{O}_3/\text{FeO}$ ratio, shown by the similarities between the chemical composition of the eclogites and the amphibolitized eclogites (Tables 1 and 2; Figs. 3b, 4 and 7b).

The prograde metamorphism in the Alpine s.s. event took place under the P-T conditions of the field bounded by curves 10 and 10' (Fig. 15). They define the stability field of barroisite, along with albite and pistacite, which replace almost all the pre-existing minerals. The replacement of the paragonitic sericite and clinozoisite aggregates (pseudomorphosing plagioclase) by an association of large flakes of white mica and poikiloblasts of albite, epidote and amphibole, suggests that the metamorphic grade at stage D was

higher than that of the previous formation of sericite during stage C. Thus the prograde path passed into the P-T field above curve 9 (Fig. 15). The formation of barroisitic amphiboles coming from or rimming glaucophane also represent an increase in pressure between the retrograde C stage of the eo-Alpine event and the prograde D stage of the Alpine s.s. one (see Fig. 13). The maximum temperature reached during stage D would have been around 580°C taking into account the pressure needed to form the barroisitic amphiboles and the presence both of stable antigorite in the serpentinites associated with the metabasites and of chloritoid, instead of staurolite, in the surrounding micaschists. Staurolite is, however, present but associated with chloritoid (curves 11 and 11') in other micaschists belonging to the underlying Caldera nappe.

During the retrograde path towards stage E barroisite became unstable and was partly replaced by actinolite, indicating that the physical conditions below curve 10' were reached. Together with actinolite, a new generation of chlorite, albite and ores, followed by the formation of green biotite, developed under greenschist-facies conditions. The degree of recrystallization during this stage, however, varies largely from place to place within the same outcrop.

Several K-Ar data of white mica from the micaschists of the metasedimentary cover of the ophiolitic nappe and from other micaschists or gneisses of different tectonic units of the Sierra Nevada Complex give ages of around 20 Ma (PUGA, 1971; PORTUGAL et al., 1988) which represent the closing of the system at 350°C. If the cooling rate for the eo-Alpine event was greater than 10°C/Ma. (CARPENA et al., 1980) stage D should have occurred between the Upper Eocene and the Lower Oligocene. This age corresponds well with that deduced for the Lepontine event in the Alps (HUNZIKER, 1974; FREY et al., 1974; SASSI and ZANETTIN, 1975; HUNZIKER and MARTINOTTI, 1984).

7. Discussion and concluding remarks

A similar succession of metamorphic facies to that proposed for the Sierra Nevada metabasites has also been suggested for other Nevado-Filábride eclogites, such as those at Lubrin (MORTEN et al., 1987) and the Sierra de Baza (GOMEZ PUGNAIRE and FERNANDEZ SOLER, 1987). Nevertheless, significant differences do exist between the mineralogy described for the Sierra de Baza and for the Sierra Nevada eclogites (PUGA et al., 1989) and also for their P-T-t evolutions.

According to GOMEZ PUGNAIRE and FERNANDEZ SOLER (1987), the different metamorphic events within the Sierra de Baza metabasites are the consequence of a single subduction process in the Upper Cretaceous during which the eclogite stage was developed. This was followed by a slow uplift period during which the pressure decreased while the temperature increased to reach the amphibolitic stage and from then on diminished to the greenschist-facies conditions. Apart from the anomaly that the rise in temperature of the tectonically exhumated slab represents (cf., e.g., SPEAR et al., 1984), our mineralogical data (omphacite-garnet KD values in the eo-Alpine event, in stable coexistence with antigorite, chloritoid and staurolite) indicate that a higher temperature was reached at the eclogitic stage than at the following amphibolitic one (B and D, Fig. 15). On the other hand, if the process is considered continuous with only one subduction phase, then the temperature decrease in the subducted slab from the Upper Cretaceous onwards would be $<3^{\circ}\text{C/Ma}$. which would be a very slow cooling rate for an Alpine chain (CARPENA et al., 1986). In fact, the K-Ar data for the white micas of the ophiolitic sequence and other units of the Sierra Nevada Complex give two groups of cooling ages at approximately 60 and 20 Ma., which is also better explained by two separate exhumation processes after the eo-Alpine and the Alpine s.s. metamorphic events, respectively. The pressure increase represented by the overgrown of glaucophane by barroisitic amphiboles (Fig. 13) is also better explained by an intermediate exhumation process between the two metamorphic events.

Other arguments that support the postulated double subduction-exhumation process are: a) the existence of two diaphthoretic stages in the greenschist facies, following the eo-Alpine and the Alpine metamorphic climaxes, which affected not only the ophiolitic nappe but also other tectonic units of the Sierra Nevada Complex (PUGA et al., 1976); b) the existence of two episodes of albitization in the Mulhacén Group of nappes due to circulation of metasomatic fluids during the distensive periods following both metamorphic events; c) the deposition upon the ophiolitic nappe of some andesitic tuffites genetically related to the eo-Alpine subduction process (PUGA et al., 1984-85) and dated as Paleocene (PORTUGAL et al., 1988), while the Neogene magmatism of the Alboran domain, which began in the Miocene, could be genetically related to the second subduction process (TORRES ROLDAN et al., 1986).

Taking into account the P-T-t path and the geological and geochronological data we conclude that the metamorphic evolution of the Sierra Nevada metabasites may well have been the result of two distinct subduction-exhumation processes, to depths of about 50 km and 30 km, during the Upper Cretaceous and the Upper Eocene-Lower Oligocene, respectively.

Acknowledgements

The authors are very grateful to Dr. J. Desmons (Nancy), Dr. Ch. Miller (Innsbruck) and Dr. RL Torres-Roldán (Granada) for critical reading of the manuscript. The support received from our Research Institutions: CSIC (Spain), MPI (Italy) and Geological Survey (Czechoslovakia) is also acknowledged. This study was partly financed by Project PB 85/408 (CAICYT, Spain).

References

BECCALUVA, L., OHNENSTETTER, D. and OHNENSTETTER, M. (1979): Geochemical discrimination between ocean-floor and island-arc tholeiites. Application to some ophiolites. *Can. J. Earth Sci.*, 16, 1874-1882.

BECCALUVA, L., PICCARDO, G.B. and SERRI, G. (1980): Petrology of northern Apennines ophiolites and comparison with other Tethyan ophiolites. In: Panayiotou, A. (ed.). *Ophiolites Proc. Int. Symp.*, Cyprus, 1979, 314-331.

BECCALUVA, L., OHNENSTETTER, D., OHNENSTETTER, M. and PAUPY, A. (1984): Two magmatic series with island arc affinities within the Vourinos ophiolite. *Contrib. Mineral. Petrol.*, 85, 253-271.

BENCE, A.E. and ALBEE, A.L. (1968): Empirical correction factors for the electron microanalysis of silicates and oxides. *Jour. Geol.*, 76, 382-403.

BOCQUET, J., DELALOYE, M., HUNZIKER, J.C. and KRUMMENACHER, D. (1974): K-Ar and Rb-Sr dating of blue amphiboles, micas and associated minerals from the Western Alps. *Contrib. Mineral. Petrol.*, 47, 7-26.

BODINIER, J.L., MORTEN, L., PUGA, E. and DIAZ DE FEDERICO, A. (1987): Geochemistry of metabasites from the Nevado-filabride Complex, Betic Cordilleras, Spain: Relics of a dismembered ophiolitic sequence. *Lithos*, 20, 235-245.

BROWN, E.H. (1977): The crossite content of Ca-amphibole as a guide to pressure of metamorphism. *J. Petrology*, 18, 53-72.

BURGOS, J., DIAZ DE FEDERICO, A., MORTEN, L. and PUGA, E. (1980): The ultramafic rocks from the Cerro del Almirez. Sierra Nevada Complex, Betic Cordilleras, Spain. Preliminary report. *Cuad. Geol.*, 11, 157-165.

CANN, J.R. (1970): Rb, Sr, Y, Zr, Nb in some ocean-floor basaltic rocks. *Earth Planet. Sci. Lett.*, 10, 7-11.

CAPREDI, S., VENTURELLI, G., BOCCHE, G., DOSTAL, J., GARUTI, G. and ROSSI, A. (1980): The geochemistry and petrogenesis of an ophiolitic sequence from Pindos, Greece. *Contrib. Mineral. Petrol.*, 74, 189-200.

CARPENA, J., POGNANTE, U. and LOMBARDO, B. (1986): New constraints for the timing of the alpine metamorphism in the internal ophiolite nappes from the western Alps as inferred from fission-track data. *Tectonophysics*, 127, 117-127.

CAWTHORN, R.G. and COLLERSON, K.D. (1974): The recalculation of pyroxene end-member parameters and the estimation of ferrous and ferric iron content from electron microprobe analyses. *Amer. Mineral.*, 59, 1203-1208.

CHIESA, S., CORTESOGNO, L. and FORCELLA, F. (1977): Caratteri e distribuzione del metamorfismo alpino nel Gruppo di Voltri e nelle zone limitrofe della Liguria occidentale con particolare riferimento al metamorfismo di alta pressione. *Rend. Soc. Ital. Mineral. Petrol.*, 33, 253-279.

CHOPIN, C. and MALUSKI, M. (1980): 39Ar/40Ar dating of high pressure metamorphic micas from the Gran Paradiso area (Western Alps): evidence against the blocking temperature concept. *Contrib. Mineral. Petrol.*, 74, 109-122.

COLEMAN, R.G., LEE, D.E., BEATTY, L.B. and BRANNOCK, W.W. (1965): Eclogites and eclogites: their differences and similarities. *Geol. Soc. Amer. Bull.*, 76, 483-508.

CORTESOGNO, L., ERNST, W.G., GALLI, M., MESSIGA, B., PEDEMONTE, G.M. and PICCARDO, G.B. (1977): Chemical petrology of eclogitic lenses in serpentinite Gruppo di Voltri, Ligurian Alps. *J. Geol.*, 85, 255-277.

DAL PIAZ, G.V. and ERNST, W.G. (1978): Areal geology and petrology of eclogites and associated metabasites of the Piamonte ophiolite nappe, Breuil-St.Jacques area, Italian Western Alps. *Tectonophysics*, 51, 99-126.

DELALOYE, M. and DESMONS, J. (1976): K-Ar radiometric age determinations of white micas from the Piemont zone, French-Italian Western Alps. *Contrib. Mineral. Petrol.*, 57, 297-303.

DESMONS, J. (1977): Mineralogical and petrological investigations of Alpine metamorphism in the internal French Western Alps. *Amer. Jour. Sci.*, 277, 1045-1066.

DIAZ DE FEDERICO, A. (1980): Estudio geológico del Complejo de Sierra Nevada en la transversal del Puerto de la Ragua, Cordillera Bética. Thesis University of Granada, 597 pp.

DIAZ DE FEDERICO, A., GOMEZ PUGNAIRE, M.T., PUGA, E. and TORRES ROLDAN, R.L. (1977): Igneous and metamorphic processes in the geotectonic evolution of the Betic Cordilleras (Southern Spain). *Cuad. Geol.*, 8, 37-60.

DIETRICH, V., VUAGNAT, M. and BERTRAND, J. (1974): Alpine metamorphism of mafic rocks. *Schweiz. Mineral. Petrogr. Mitt.*, 54, 291-323.

EGEGER, C.G. (1963): On the tectonics of the eastern Betic Cordilleras (SE Spain). *Geol. Rundes.*, 53, 260-269.

ELLIS, D.J. and GREEN, D.H. (1979): An experimental study of the effect of Ca upon garnet-clinopyroxene Fe-Mg exchange equilibria. *Contrib. Mineral. Petrol.*, 71, 13-22.

ERNST, W.G. (1979): Coexisting sodic and calcic amphiboles from high-pressure metamorphic belts and the stability of barroisite amphibole. *Mineral. Mag.*, 43, 269-278.

ESSENE, E.J. and FYFE, W.S. (1967): Omphacite in Californian metamorphic rocks. *Contrib. Mineral. Petrol.*, 63, 621-640.

EVANS, B.W., JOHANNES, W., OTERDOOM, H. and TROMMSDORFF, V. (1976): Stability of Chrysotile and Antigorite in the serpentinite multisystem. *Schweiz. mineral. petrogr. Mitt.*, 56, 79-93.

FALLOT, P., FAUVERMURET, A., FONTBOTE, J.M., and SOLE SABARIS, L. (1961): Estudios sobre las series de Sierra Nevada y de la llamada Mischungszone. *Bol. Inst. Geol. Min. España*, 71, 345-557.

FRANZ, G. and ALTHAUS, E. (1977): The stability relations of the paragenesis paragonite-zoisite-quartz. *N. Jb. Miner. Abh.*, 130, 159-167.

FRANZINI, M., LEONI, L. and SAITA, M. (1972): A simple method to evaluate the matrix effects in X-ray fluorescence analysis. *X-Ray Spectrom.*, 1, 151-154.

FRANZINI, M., LEONI, L., and SAITA, M. (1975): Revisione di una metodologia analitica per fluorescenza X basata sulla correzione completa degli effetti di matrice. *Rend. Soc. Ital. Mineral. Petrol.*, 31, 365-378.

FREY, M., HUNZIKER, J.C., FRANK, W., BOCQUET, J., DAL PIAZ, G.V., JÄGER, E. and NIGGLI, E. (1974): Alpine metamorphism of the Alps. A review. *Schweiz. Mineral. Petrogr. Mitt.*, 54, 247-290.

GOMEZ PUGNAIRE, M.T. and FERNANDEZ SOLER, J.M. (1987): High-pressure metamorphism from the Betic Cordilleras (SE Spain) and its evolution during the Alpine orogeny. *Contrib. Mineral. Petrol.*, 95, 231-244.

HEBEDA, E.H., BOELZIJK, N.A.I.M., PRIEM, H.N.A., SIMON, O.J., VERDUZMEN, E.A.TH. and VERSCHEURE, R.M., (1977): Excess radiogenic Ar versus undisturbed Rb-Sr systems in unaltered dolerite relicts within Late Jurassic metabasites in the Alpine belt of SE Spain. E.C.O.G., Pisa (Italy). September 1975.

HOLLAND T.J.B. (1979): Experimental determination of the reaction paragonite=jadeite+kyanite+H₂O, and internally consistent thermodynamic data for part of the system Na₂O-Al₂O₃-SiO₂-H₂O, with applications to eclogites and blueschists. *Contrib. Mineral. Petrol.*, 68, 292-301.

HOSCHEK, G. (1969): The stability of staurolite and chloritoid and their significance in metamorphism of pelitic rocks. *Contrib. Mineral. Petrol.*, 22, 208-232.

HUNT, J.A. and KERRICK, D.M. (1977): The stability of sphene, experimental redetermination and geologic implications. *Geochim. Cosmochim. Acta*, 41, 279-288.

HUNZIKER, J.C. (1974): Rb-Sr and K-Ar age determination and the alpine tectonic history of the Western Alps. *Mem. Ist. Geol. Miner. Univ. Padova*, 31, 1-56.

HUNZIKER, J.C. and MARTINOTTI, G. (1984): Geochronology and evolution of the Western Alps: A review. *Mem. Soc. Geol. It.*, 29, 43-56.

KUSHIRO, I. (1969): Clinopyroxene solid solutions formed by reaction between diopside and plagioclase at high pressure. *Miner. Soc. Am. Spec. Paper*, 2, 179-191.

LEONI, L. and SAITA, M. (1976): X-ray fluorescence analysis of 29 trace elements in rock and mineral standards. *Rend. S.I.M.P.*, 32, 497-510.

LEAKE, B.E. (1978): Nomenclature of amphiboles. *Amer. Miner.*, 63, 1023-1052.

MARESCH, W.V. (1977): Experimental studies on glauconophane: an analysis of present knowledge. *Tectonophysics*, 43, 109-125.

MESSIGA, B., PICCARDO, G.B. and ERNST, W.G. (1983): High-pressure eo-alpine parageneses developed in magnesian metagabbros, Gruppo di Voltri, Western Liguria, Italy. *Contrib. Mineral. Petrol.*, 83, 1-15.

MIYASHIRO, A. (1973): The Troodos ophiolitic complex was probably formed in an island arc. *Earth. Planet. Sci. Letter*, 19, 218-224.

MONVISO, (1980): The Monviso ophiolite complex. In: *Ophiolites Proc. Int. Symp. Cyprus*, 1979. Ed. A. Panayiotou, 332-340.

MORTEN, L., BARGOSSI, G.M., MARTINEZ MARTINEZ, J.M., PUGA, E. and DIAZ DE FEDERICO, A. (1987): Metagabbro and associated eclogites in the Lubrin area, Nevado-Filabride Complex, Spain. *J. Metamorphic Geol.*, 5, 155-174.

MOTTANA, A., BOCCHIO, R. (1975): Superferric eclogites of the Voltri Group (Pennidic Belt, Appennines). *Contrib. Mineral. Petrol.*, 49, 201-210.

NEWTON, R.C. and KENNEDY, G.C. (1963): Some equilibrium reaction in the join CaAl₂Si₂O₈-H₂O. *J. Geophys. Res.*, 68, 2967-2983.

NITSCH, K.H. (1974): Neue Erkenntnisse zur Stabilität von Lawsonit. *Fortschr. Mineral.*, 51, 34-35.

PEARCE, J.A. (1980): Geochemical evidence for the genesis and eruptive setting of lavas from Tethyan ophiolites. In: Panayiotou, A. (ed.) *Ophiolites Proc. Intern. Ophiolite Symp.*, Cyprus 1979, 261-272.

PEARCE, J.A. and CANN, J.R. (1973): Tectonic setting of basic volcanic rocks determined using trace element analyses. *Earth Planet. Sci. Letter*, 19, 290-300.

POGNANTE, U. (1985): Coronitic reactions and ductile shear zone in eclogitized metagabbro, Western Alps, North Italy. In: Smith, D.C., Franz, G., and Gebauer, D. (eds.). *Chemistry and Petrology of eclogites*. *Chem. Geol.*, 50, 99-109.

PORTUGAL FERREIRA, M., FERREIRA, J.T., PUGA, E. and DIAZ DE FEDERICO, A. (1988): Geochronological contribution to the petrogenetic picture of the Betic Chain (SE Spain). *II Congreso Nacional de Geología de España. Comunicaciones* 2, 55-58.

PUGA, E. (1965): Nuevos datos sobre las anfibolitas del borde NW de Sierra Nevada. *Not. Comun. Inst. Geol. Min. España*, 80, 137-156.

PUGA, E. (1971): Investigaciones petrológicas en Sierra Nevada occidental. Thesis, University of Granada, 269 p.

PUGA, E. (1977): Sur l'existence dans le complexe de la Sierra Nevada (Cordillère Bétique, Espagne du Sud) d'éclogites et sur leur origine probable à partir d'une croûte océanique mésozoïque. *C. R. Acad. Sci. Paris*, 285, 1379-1382.

PUGA E. (1980): Hypothèses sur la genèse des magmatismes calcoalcalins, intra-orogénique et postorogénique alpins, dans les Cordillères bétiques. *Bull. Soc. geol. France*, 7, 243-250.

PUGA E. and DIAZ DE FEDERICO, A. (1976): Metamorfismo polifásico y deformaciones alpinas en el Complejo de Sierra Nevada (Cordillera Bética). Implicaciones geodinámicas. Reunión Geodinámica Cordillera Bética y Mar de Alborán (Granada, mayo 1976), 79-111.

PUGA, E. and DIAZ DE FEDERICO, A. (1984): Materiales indicativos de una asociación ofiolítica en el Complejo de Sierra Nevada y su significado geodinámico. Informes Reunión Científica Proyecto C-40010/8 sobre El borde mediterráneo español, 21-22.

PUGA, E., DIAZ DE FEDERICO, A. and FONTBOTE, J.M. (1974): Sobre la individualización y sistematización

de las unidades profundas de la Zona Bética. *Estud. Geol.*, 30, 543-548.

PUGA, E., DIAZ DE FEDERICO, A., MORTEN, L. and BARGOSSI, G.M. (1984-85): La Formación de Sopotújar del Complejo de Sierra Nevada. Caracterización petrológica y geoquímica. *Cuad. Geol.*, 12, 61-89.

PUGA, E., FEDIUKOVA, E., DIAZ DE FEDERICO, A. and MORTEN, L. (1989): The mineral parageneses and mineralogical evolution of the ophiolitic eclogites and related rocks from the Sierra Nevada (Betic Cordillera, Southeastern Spain). *Bol. Soc. Esp. Mineral.*, 12, 189-211.

PURDY, J.W. and JÄGER, E. (1976): K-Ar ages on rock-forming minerals from the Central Alps. *Mem. Ist. Geol. Miner. Univ. Padova*, 30, 1-31.

RICHARDSON, S.W., GILBERT, M.C. and BELL P.M. (1969): Experimental determination of kyanite-andalusite and andalusite-sillimanite equilibria: the aluminium silicate triple point. *Am. J. Sci.*, 267, 259-272.

ROBINSON, P., SPEAR, F.S., SCHUMACHER, J.C., LAIRD, J., KLEIN, C., EVANS, B.W. and DOOLAN, B.L. (1982): Phase relations of metamorphic amphiboles: natural occurrence and theory. In: VEBLEN, D.R. and RIBBE, P.H. (eds.) *Amphiboles: Petrology and experimental phase relations. Reviews in Mineralogy*, 9B. *Miner. Soc. Amer.*, 1-227.

SASSI, F.P. and ZANETTIN, B. (1975): Metamorphic history of the Eastern Alps. In: DAL PIAZ et al. *Geological outline of the Italian Alps, Geology of Italia*. *Earth Sci. Soc. Libyan Arab. Rep.*

SCARFE, C.M. and WYLLIE, P.J. (1967): Serpentine dehydration curves and their bearing on serpentine deformation orogenesis. *Nature* 215, 945-946.

SERRI, G. (1980): Chemistry and petrology of gabbroic complexes from the Northern Apennine ophiolites. In: PANAYIOTOU, A. (ed.) *Ophiolites Proc. Int. Symp. Cyprus*, 1979, 781.

SHERVAIS, J.W. (1982): Ti-V plots and the petrogenesis of modern and ophiolitic lavas. *Earth Planet. Sci. Letter*, 59, 101-108.

SMEWING, J.D. and POTTS, Ph.J. (1976): Rare-earth abundances in basalts and metabasalts from the Troodos Massif, Cyprus. *Contrib. Mineral. Petrol.* 57, 245-258.

SMULIKOWSKI, K. (1965): Chemical differentiation of garnets and clinopyroxenes in eclogites. *Bull. Acad. Poloniae des Sci.*, VIII, 1.

SPEAR, F.S., SELVERSTONE, J., HICKMOTT, D., CROWLEY, P. and HODGES, K.V. (1984): P-T paths from garnet zoning: A new technique for deciphering tectonic processes in crystalline terranes. *Geology*, 12, 87-90.

TORRES ROLDAN, R.L., POLI, G. and PECERILLO, A. (1986): An early miocene arc-tholeiitic magmatic dike event from the Alboran Sea. Evidence for precollisional subduction and back-arc crustal extension in the westernmost Mediterranean. *Geol. Rundsch.*, 75, 219-234.

TRÜMPY R. (1973): *The timing of orogenic events in the Central Alps: Gravity and tectonics*. Wiley, New York, 229-251.

VENTURELLI, G., CAPEDRI, S., THORPE, R.S. and POTTS, P.J. (1979): Rare-Earth and other element distribution in some ophiolitic metabasalts of Corsica, Western Mediterranean. *Chem. Geol.*, 24, 339-353.

VENTURELLI, G., THORPE, R.S. and POTTS, P.J. (1981): Rare earth and trace element characteristics of ophiolitic metabasalts from the Alpine-Apennine belt. *Earth Planet. Sci. Letter*, 53, 109-123.

WINCHESTER, J.A. and FLOYD, P.A. (1977): Geochemical discrimination of different magma series and their differentiation products using immobile elements. *Chem. Geol.*, 20, 325-343.

WOOD, D.A., TARNEY, J., VARET, J., SAUNDERS, A.D., BOUGAULT, H., JORON, J.L., TREUIL, M. and CANN, J.R. (1979): Geochemistry of basalts drilled in the North Atlantic by IPOD LEG 49: Implications for mantle heterogeneity. *Earth Planet. Sci. Letter*, 42, 77-97.

ZERMATTEN, H.L.J. (1929): *Geologische onderzoeken in de randzone van het venster der Sierra Nevada* (Spanje). Thesis Delft, 104 p.

Manuscript received April 4, 1988; revised manuscript accepted June 27, 1989.